Progress In Electromagnetics Research, PIER 46, 33–75, 2004

PERIODIC OPEN RESONATORS: PECULIARITIES OF PULSE SCATTERING AND SPECTRAL FEATURES

A. Perov, Y. Sirenko, and N. Yashina

Institute of Radiophysics and Electronics
National Academy of Sciences of Ukraine
12, Ak. Proskury St., Kharkov, 61085, Ukraine

Abstract—The approach based on investigation of characteristic properties of the resolving operators (resolvents) of stationary boundary value problems of the theory of wave diffraction by gratings is used for the analysis of the basic regularities running the formation of resonant non-stationary scattered fields. Information about singularities provides the description of the anomalous effects connected with possibility of existence, in the structures under consideration, of eigen modes having super high Q-factor, with linear "interaction" of modes in the parameter regions of spectrum crowding.

1. INTRODUCTION

Various resonant phenomena make the essence of electromagnetic processes, especially in electromagnetic wave scattering. The knowledge about the reasons and their nature can help to run resonant phenomena and to use them in various engineering developments. When investigating electromagnetic wave scattering characteristics for gratings one has to obtain reliable results with rather high accuracy determination of resonance, those mainly reflect rather subtle features of the object.

The problems that are connected with theoretical study and analytical description of physical nature of various resonant and anomalous time-space field transformations can not be solved by means of traditional approaches and techniques. The necessity of efficiency of their solution arrives to the analyzing of analytical continuation of the diffraction problem solutions into domain of complex parameter values. The singularities (poles and branch points of analytic continuation of the diffraction problem solution into complex parameter domain) determine the spectral characteristics of the structures under consideration as open periodic resonators. Their "shadows" appears usually when parameters are varying within domain of real values (diffraction theory), but their significance in formation of structure's response to any external excitation is predestining. The approach, based on the investigation of singularities (spectrum) of resolving operators of stationary boundary value problems in theory of wave diffraction by open periodic resonators [1] (gratings), enables to consider on the common methodological base various mathematical, physical and applied problems of the theory of resonant wave scattering.

Its advantages are to be demonstrated in this paper for model problem depicted in Fig. 1, performing resonant phenomena, which are of wide use in different scientific and engineering areas. Herein we are to demonstrate and treat the influence of elements of complex spectrum of periodic resonators onto pulse scattering features.

The resonant character of the phenomena under investigation in the paper put certain requirements to the methods and approaches, used for their study. Clear that the only reliable tools in the situation are rigorous methods and corresponding numerical algorithms providing results with required accuracy without limitations of parameter region. The efficiency of methods of analytical regularization in FD has been already verified for such situation [1–3]. These methods exploit the classic for the functional analyses and theory of integral equation idea of explicit inversion of singular terms

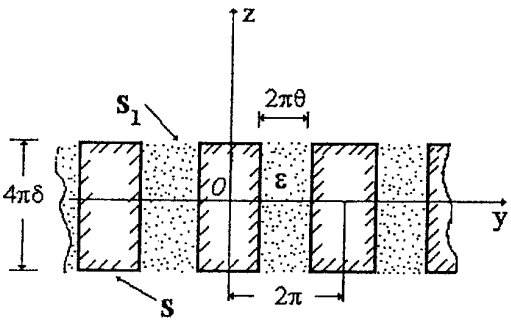

Figure 1. Configuration of grating.

of ill- posed operator equation of the first kind. Wave scattering phenomena (in TD) are investigated by means of TD transform operator method, also exploiting semi inversion technique and FDTD schemas with accurate restriction of computational domain [4–6].

2. BASIC MODEL PROBLEM AND DIFFRACTION RESONANCE MODES IN FD

1. Consider following model problem. Let plane E-polarized wave

$$\tilde{U}^i(g;\kappa) = \exp[i(\Phi_0 y - \Gamma_0(z - 2\pi\delta))], \quad z \geq 2\pi\delta.$$

is incident to grating (Fig. 1; the structures are homogeneous along x axis). Total diffraction field is determined by

$$\tilde{U}(y,z) \in C^2(Q) \cap C^1(\overline{Q})$$

that is solution of a two-dimensional Helmholtz equation

$$\left[\frac{\partial^2}{\partial y^2} + \frac{\partial^2}{\partial z^2} + \kappa^2\varepsilon\right]\tilde{U}(g;\kappa) = 0; \quad g = \{y,z\} \in Q, \quad \kappa > 0, \tag{1}$$

satisfying the radiation condition

$$\tilde{U}(y,z) = \left\{\begin{array}{c}\tilde{U}^i\\ 0\end{array}\right\} + \sum_{n=-\infty}^{\infty}\left\{\begin{array}{c}a_n\\ b_n\end{array}\right\} e^{i(\Phi_n y \pm \Gamma_n(z \mp 2\pi\delta))}, \quad \left\{\begin{array}{c}z > 2\pi\delta\\ z < -2\pi\delta\end{array}\right\}, \tag{2}$$

matched with the requirement do not consider in the scattered field waves coming from $z = \pm\infty$, and the generalized boundary conditions

$$\tilde{U}\left\{\frac{\partial\tilde{U}}{\partial y}\right\}(y + 2\pi, z) = e^{i2\pi\Phi}\tilde{U}\left\{\frac{\partial\tilde{U}}{\partial y}\right\}(y,z); \tag{3}$$

$$\tilde{U}\Big|_s = 0; \int\limits_v \left(\left|\tilde{U}\right|^2 + \left|\mathrm{grad}\tilde{U}\right|^2 \right) d\nu < \infty.$$

Here κ is a dimensionless frequency parameter that is the ratio of the grating period and the exciting wavelength. All processes are considered in dimensionless (having meaning of a length) space-time coordinates $\{x, y, z; t\}$, in terms of which the length of the grating period is equal to 2π, and time dependence is defined by factor $e^{(-i\kappa t)}$; $\varepsilon \geq 1$ is a real constant that describes the relative permittivity of the grating material; $Q = R^2 \backslash (S_1, \cup\, int\ S)$; S_1, and $S - 2\pi$ — are periodic contours piecewise smooth in which specify the lines of ε break and the boundaries of perfectly conducting scatters. R^2 is a plane of variables y, z; C^m is the class of the continuously differentiable functions up to the m-th order, inclusively; $\Phi_n = n + \Phi$, $\Gamma_n = (\kappa^2 - \Phi_n^2)^{1/2}$, $\mathrm{Re}, \mathrm{Im}\Gamma_n \geq 0$; V is an arbitrary compact in Q; δ and Φ are real parameters; $\tilde{U}(y, z) = E_x$ — is the only non-zero component the electric field.

2. Space harmonic's complex-valued amplitudes a_n and b_n forming the diffraction field (2) are complicated functions of κ, Φ, geometry of grating and media parameters. For the far zone analyses of scattered field far not all amplitudes are of the same importance. Clear that only propagating modes with numbers n such that $\mathrm{Re}\Gamma_n \geq 0$ are forming far zone field. $N = \sum\limits_n \frac{\mathrm{Re}\Gamma_n}{|\Gamma_n|}$ — is the number of harmonics propagating in free space, M defines regime of coupling of regions $|z| \geq 2\pi\delta$ and is equal to the number of propagating H_{0m} waves in the waveguide channels $|z| \leq 2\pi\delta$, $\pi(1-\theta) \leq y - 2\pi s \leq 2\pi - \pi(1-\theta)$, $s = 0, \pm 1 \ldots$. The couple of these values $\{N, M\}$ is the important characteristic of wave diffraction by grating. Various combination of N and M define the scattering regime and enable to predict resonance and anomalous diffraction phenomena (FD) such as complete reflection and transmission of plane waves by transparent grating and complete Non-specula reflection of plane waves by reflecting grating and etc. [1, 7]. Spectral theory [1] discovered the principal issues of nature and routines of implementation of various resonant regimes. This theory revealed one-to-one correspondence between diffraction resonance and eigen frequencies. Spectral theory also defined personal or collective influence of "natural resonance" (free oscillations or eigen modes) that occurred in non physic complex frequencies κ, that are elements of discrete spectral set Ω_κ, onto diffraction regimes. In this set homogeneous problem (1)–(3) with $\tilde{U}^i \equiv 0$ has non-trivia! solutions. In such a way the principal features of spectrum Ω_κ and corresponding frequency selective properties of gratings have been investigated and dynamic pictures of them have been portrayed [1, 7].

3. TRANSITION INTO TD. RELATION OF STATIONARY AND NON-STATIONARY SIGNALS

Let the solution of diffraction problem (1)–(3) (a certain of the diffraction characteristics $f(\kappa)$) be known in some frequency κ band. Now we are concerned with the question how the peculiarities of resonant wave scattering processes, which are observed in the frequency domain [1, 2, 7], will make–themselves evident in the time domain. Such individual impact of an anomalous and resonant mode of scattering is easy to observe by windowing procedure. The reasonably narrow-band "window" $f_0(\kappa)$ is put on the characteristic $f(\kappa)$ (on the wave $\tilde{U}^i$ of excitation in the plane $z = 2\pi\delta$). Image of $f(\kappa)$ in the time domain (a characteristic $F(t)$) is derived with the help of integral Fourier transform

$$F(t) = \int\limits_{-\infty}^{\infty} f(\kappa) f_0(\kappa) e^{-i\kappa t} d\kappa$$

Relationships of the type

$$f_0(\kappa) = \frac{1}{2\pi} \int\limits_{-\infty}^{\infty} F_0(t) e^{i\kappa t} dt \leftrightarrow F_0(t) = \int\limits_{-\infty}^{\infty} f_0(\kappa) e^{-i\kappa t} d\kappa$$

establish correspondence between the stationary and non-stationary signals, in particular between the signals exciting the grating. With a choice

$$f_0(\kappa) = e^{-\alpha^2(\tilde{\kappa}-\kappa)^2} e^{iT\kappa}, \quad \alpha > 0, \quad \mathrm{Im}T = 0, \tag{4}$$

$\tilde{\kappa}$ being the center (carrying) frequency, we obtain

$$F_0(t) = e^{-i\tilde{\kappa}(t-T)} \frac{\pi^{1/2}}{\alpha} e^{-(t-T)^2/4\alpha^2}, \tag{5}$$

where $\tilde{\kappa}$ determines now the high-frequency filling of a signal, and the quantity T determines the time of delay. A requirement

$$T > 0, \quad |F_0(0)|/|F_0(T)| = const \ll 1 \tag{6}$$

relates the starting of "contact" of a signal with the structure to the time moment $t = 0$. We should emphasis that here the term "signal" (as it differs from [8]) is used regardless of the analytical properties of the complex envelops as functions of frequency or time. The magnitude of the constant in (6), as well as the magnitude of the parameter α specifying the spectral structure of the signal F_0 is determined by conditions of computational experiment, in particular, by the effective band width of the resonance of the characteristic $f(\kappa)$ in the frequency domain that are of interest.

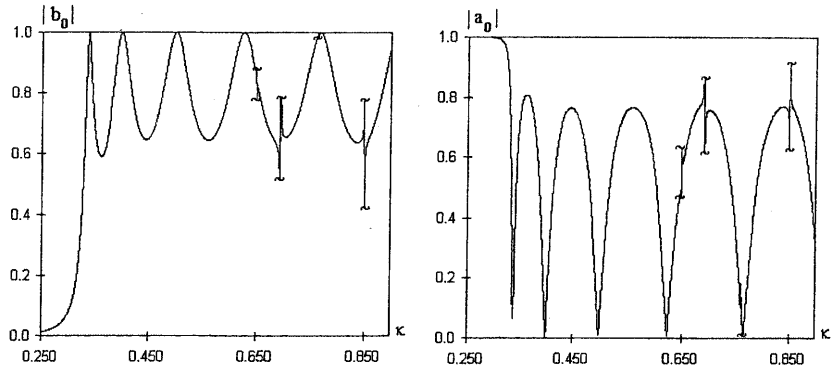

Figure 2. Transparency of the grating in frequency region κ, corresponding to regimes $\{1,1\}$ and $\{1,2\}$.

4. RESULTS OF NUMERICAL EXPERIMENTS

1. Consider first Fig. 2, where modules of coefficients both of transmission ($|b_0(\kappa)|$) and of reflection ($|a_0(\kappa)|$) for a grating made of perfectly conducting beams ($\theta = 0.8$; $\varepsilon = 3.89$; $\delta = 0.75$; $\Phi = 0.1$). are shown. The resonant response of a plane E-polarized wave of a unit amplitude up to the critical point of the H_{02}-wave ($\kappa \approx 0.634$), is coursed by resonance connected with existence of H_{01n}-type eigen modes (H_{0m} means the type of wave in connection channel, dominating in eigen field, n indicates the number of field variation along structure height $|z| \leq 2\pi\delta$) and making a incident wave possible to pass into the zone $z < -2\pi\delta$ without reflection. Above the point specified (the $\{1,2\}$ regime) there are both pure and coupled ($\kappa = 0.76$) resonance at H_{01}- and H_{02}-waves, which open and lock the Floquet's channel R completely. Within the scale accepted for Fig. 2 far not all details of the behavior of the curves $|b_0(\kappa)|$ and $|a_0(\kappa)|$ can be traced. Here the plots are terminated in the places designated by wavy lines, and the details necessary for the following are given in Figs. 3–7.

2. A narrow band pulse $F_0(t)$ (envelopes of excitation signals in both frequency and time domains are plotted in Figs. 3–7 by dashed lines) with the carrier frequency κ from the domain $\{1,1\}$ passes through the grating (we examine a pulse $B_0(t) \leftrightarrow b_0(\kappa)f_0(\kappa)$ i.e., the fundamental partial component of the non-stationary field in the plane $z = -2\pi\delta$) practically without distortion (see Fig. 3, the lower line of pictures). Change of $\arg b_0(\kappa)$ provides a physically correct delay in terms of observation time of perturbation in the transmission domain of structure ($\Delta t = 4\pi\delta\sqrt{\varepsilon}$). The high frequency filling is practically the

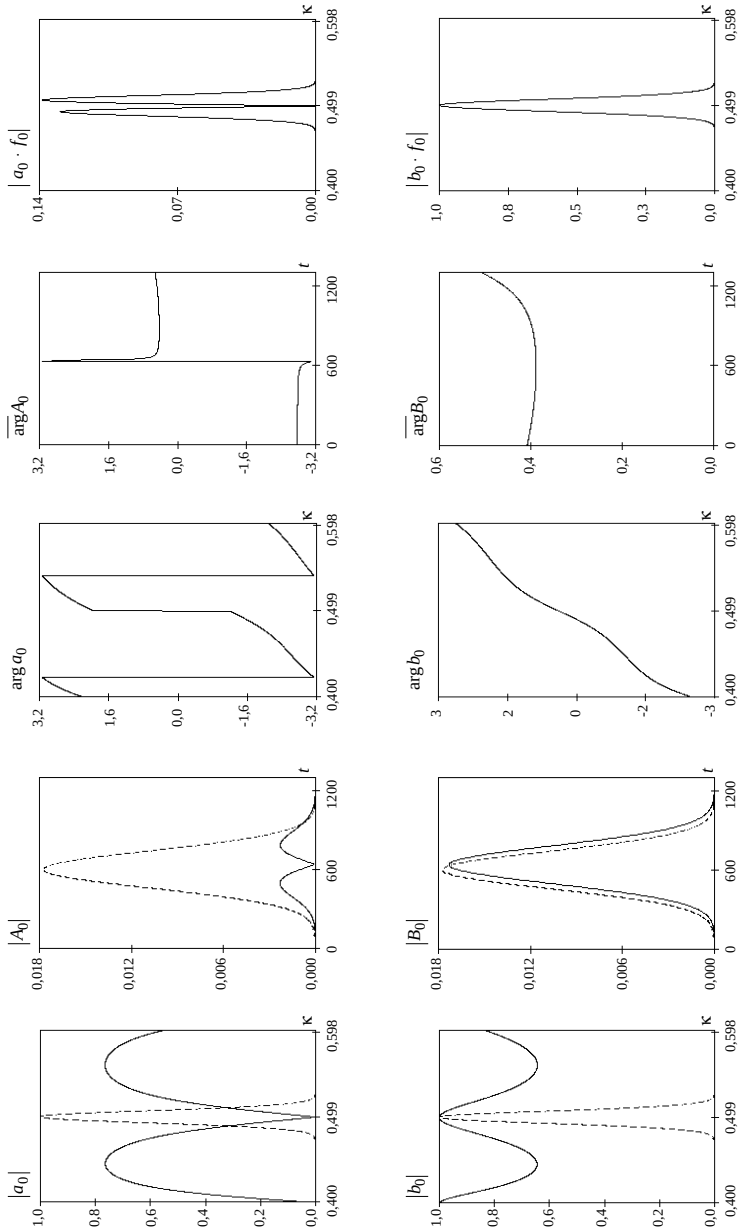

Figure 3. Reflection and transmission coefficients of the narrow band pulse with spectral content from the region $\{1,1\}$: $\alpha = 100$; $\tilde{\kappa} = 0.499$.

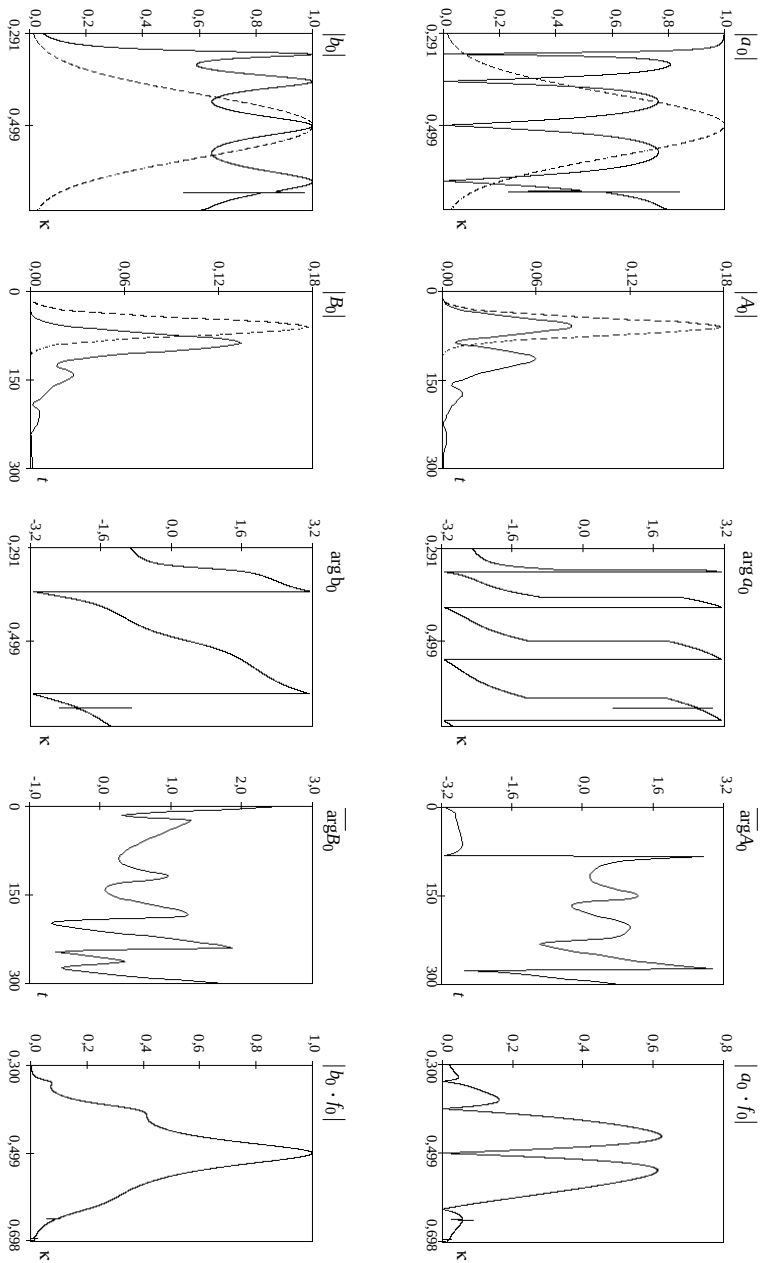

Figure 4. Grating in the field of narrow band pulse of shorter duration: $\alpha = 10$; $\tilde{\kappa} = 0.499$.

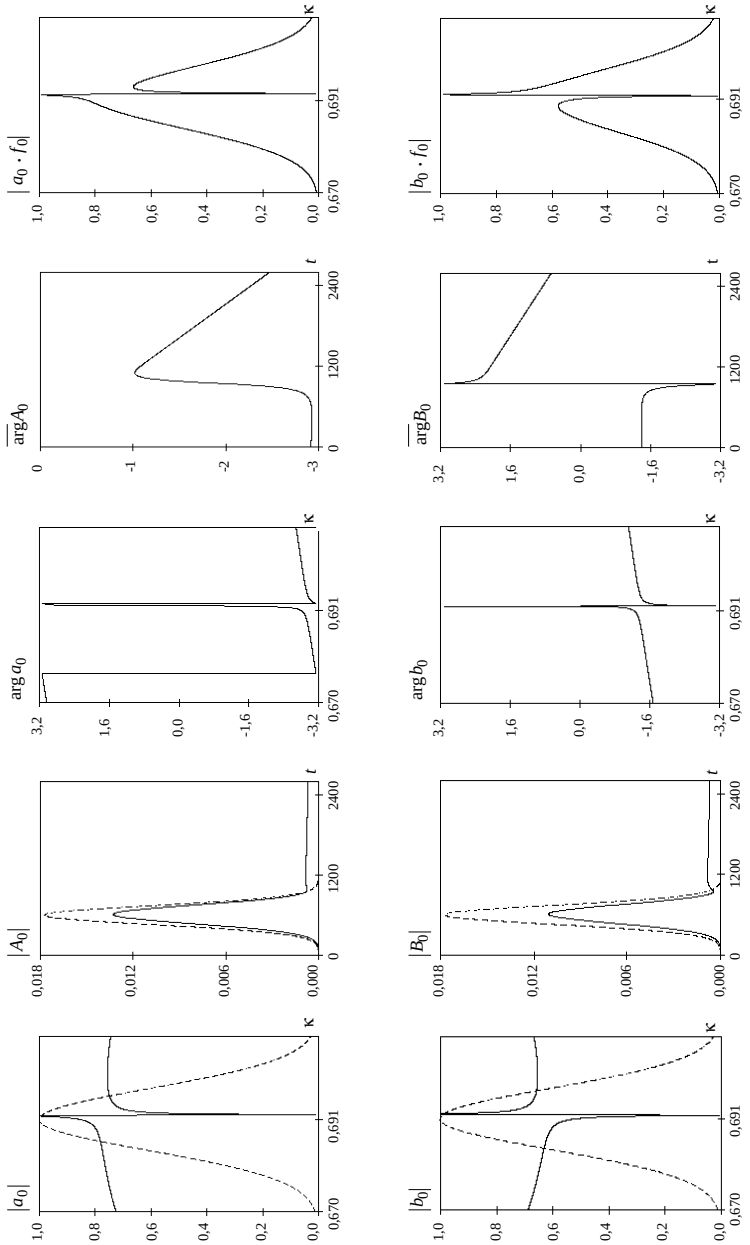

Figure 5. Reflection and transmission of the narrow band pulse with spectrum from the region $\{1, 2\}$: $\alpha = 100$; $\tilde{\kappa} = 0.691$ is close to the real-part of H_{02n}-mode eigen frequency.

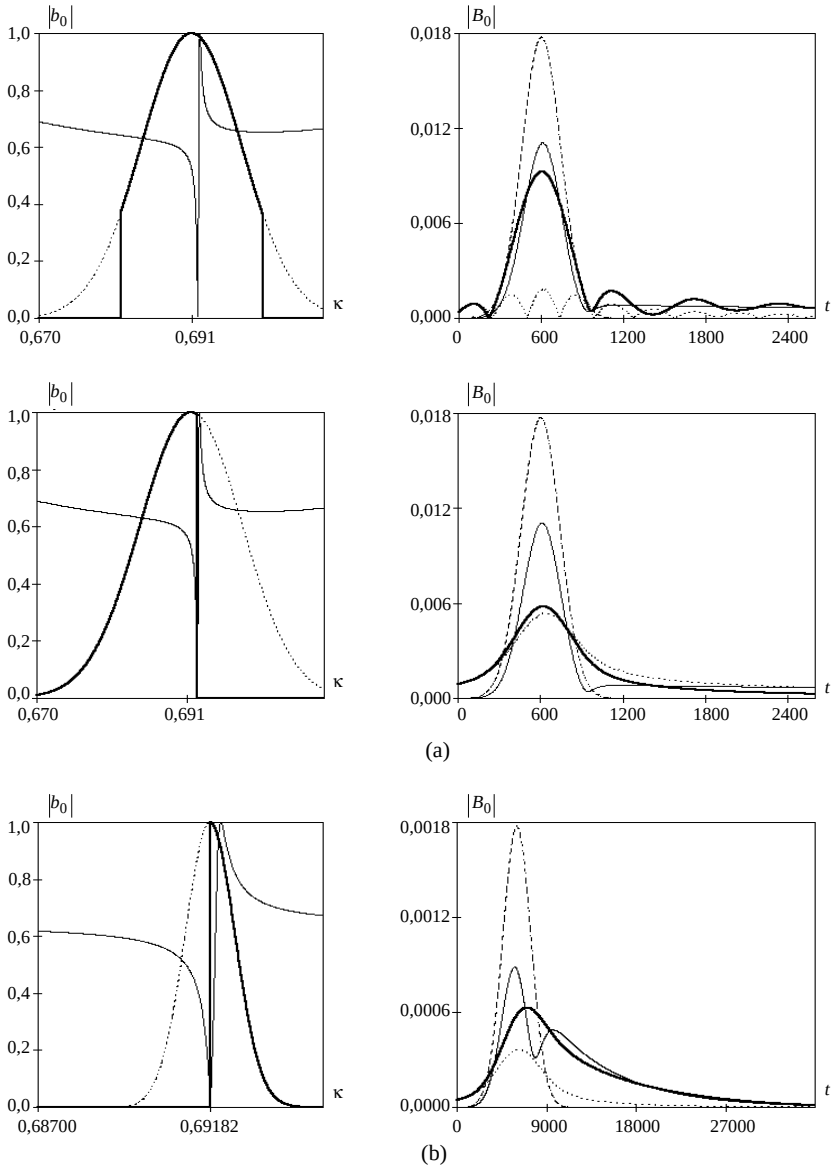

Figure 6. Response of the grating to the spectral content of pulse changing: a) $\tilde{\kappa} = 0.691$, $\alpha = 100$; b) $\tilde{\kappa} = 0.69182$, $\alpha = 1000$.

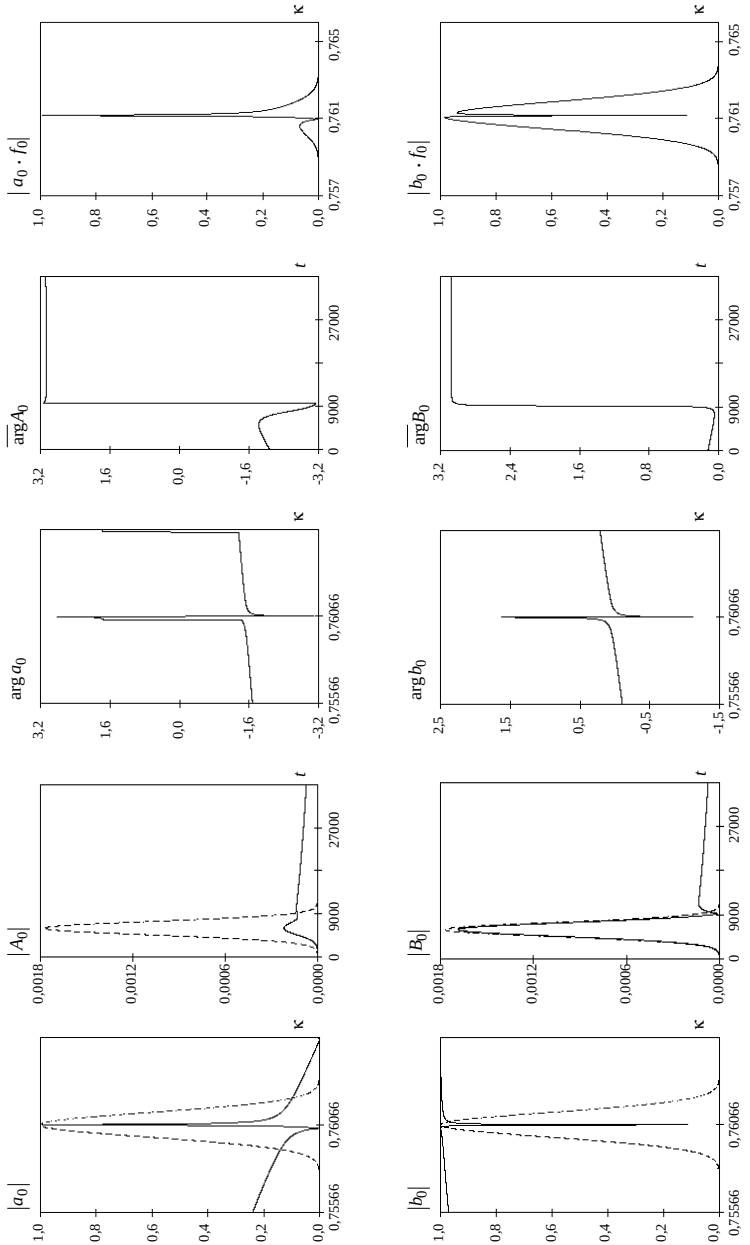

Figure 7. Reflection and transmission of the narrow pulse with spectrum covering the region of complex resonance of H_{01} and H_{02}-waves: $\tilde{\kappa} = Q76066$, $\alpha = 1000$.

same on the hole at all the time-length of the pulse as the behavior of function $\overline{\arg}B_0(t)$ shows (here and further $\overline{\arg}F(t) = \arg F(t)e^{i\tilde{\kappa}(t-T)}$). When the amplitude center $f_0(\kappa)$ does not coincide with the frequency point of total transmission regime of a plane monochromatic wave, considerable changes can take place only in the energetic characteristics of the pulse. The level of absolute values of its spectral components will be lowered.

The spectral amplitudes of a pulse $A_0(t) \leftrightarrow a_0(\kappa)f_0(\kappa)$ produced by the signal $F_0(t)$ in the reflection zone of the periodic structure are almost by an order of magnitude less (See Fig. 3, top row of fragments). The mode of complete transmission bisects its amplitude center while not changing the high-frequency filling. The pulse amplitude in its "waist" getting in the pulse's middle falls to zero. This fact is evidenced by a phase $\overline{\arg}A_0(t)$ jump equal to π in magnitude. The qualitative analytical description of "what is going on" makes possible to give the following approximate representation

$$a_0(\kappa) \approx K \sin\left[(\kappa - \tilde{\kappa})\, T_H\right] e^{i\kappa T_D}, \tag{7}$$

taking into account all the $a_0(\kappa)$ behavior peculiarities in the spectral domain of the pulse $F_0(t)$: the absolute value of local extremes (a real number K); places of $|a_0(\kappa)| = 0$ and jumps of the phase $\arg a_0(\kappa)$ by 180° (a real number T_H here its estimated value is equal 32); linear change of the phase $\arg a_0(\kappa)$ in the area of carrying frequency $\kappa = \tilde{\kappa}$ (a real number $T_D \approx 30$). Using Eq. (7) we obtain

$$A_0(t) \approx \frac{K\pi^{1/2}}{2i\alpha} e^{-i\tilde{\kappa}(t-T-T_D)} \left[e^{-(t-T-T_D-T_H)^2/4\alpha^2} - e^{-(t-T-T_D+T_H)^2/4\alpha^2}\right] \tag{8}$$

The formula (8), in turn, gives practically exact description of the pulse in the grating reflection zone: the zero value of $|A_0(t)|$ in the point $t = T + T_D$; the position of the bifurcated amplitude center; the phase variation $\overline{\arg}A_0(t)$ by 180°, etc.

The parameter α value decrease essentially shortens the duration of the excitation pulse $F_0(t)$ (See Fig. 4) and extends the bandwidth engaged by it. This band already includes some points where the modes of resonant complete transmission of plane monochromatic waves are realized as well as it partially covers the domain $\{1, 2\}$. Here the resonance on H_{02}-waves maximally expand the range of possible values of the diffraction characteristics $a_0(\kappa)$ and $b_0(\kappa)$, so the regimes of total structure transparency here can be followed by regimes of total reflection of plane waves. The pulse $F_0(t)$ is predictably (according to presentation (8)) deformed in reflection and transmission: the amplitude center of the reflected pulse is bifurcated as well as in

the previous case, but the time duration of the signal is extended appreciably. This is because under the value $\alpha = 10$, the values of T, T_H, and T_D become close to each other ($T \approx 60$), and only the forward (up to the pulse "waist") part of the reflected pulse can be placed on the interval t of the effective length of the excitation pulse $F_0(t)$. According to (8), the high-frequency filling of $A_0(t)$ is not to be changed essentially. This is valid for its front part (See the fragment with $\overline{\arg} A_0(t)$) and does not hold for its gradually attenuating tail. The last- named feels the influence of the resonance on H_{02}-wave getting into the spectral band of the excitation pulse, which has been neglected by the formula (7).

3. The shift of the carrier frequency $\tilde{\kappa}$ onto the resonance of the domain $\{1, 2\}$ changes the picture of all that is going on rather sharply. A pure resonance on H_{02}-wave of the channel of coupling (See Fig. 5) results in formation of pulses $A_0(t)$ and $B_0(t)$ in the zones of reflection and transmission, the body of which differs slightly from the excitation pulse $F_0(t)$: the energy spectrum is weakened, but the high-frequency filling has preserved. The bodies are followed by a tail slightly damping in time, high frequency filling of which does differ, even if a little, from the filling of $F_0(t)$ and remains practically constant. A basis for the description of all that is going gives the single pole representations, (See [1], formula (5.17)), which are valid in a small vicinity of the isolated complex singular point of the resolvent of the stationary boundary value problem. Let us use one of them and present the spectral components of the pulse $A_0(t)$ as

$$a_0(\kappa) f_0(\kappa) = \frac{1}{2} f_0(\kappa) \left[e^{i \arg C} + e^{i \arg D} \right] - i\beta e^{i \arg D} \left[\frac{f_0(\kappa)}{\kappa - \tilde{\kappa}_1 + i\beta} \right] \quad (9)$$

Here C and D are complex numbers (See [1], formula (5.17)); $\overline{\kappa} = \tilde{\kappa}_1 - i\beta$ — is eigen frequency of H_{02n} eigen mode of the channel of coupling between the zones of reflection and those of transmission. From Eq. (9), it is derived

$$\begin{aligned} A_0(t) &= \frac{1}{2}(e^{i \arg C} + e^{i \arg D}) F_0(t) - i\beta e^{i \arg D} \int\limits_{-\infty}^{+\infty} \frac{f_0(\kappa)}{\kappa - \tilde{\kappa}_1 + i\beta} e^{-i\kappa t} d\kappa \\ &= A_{0,1}(t) + A_{0,2}(t). \end{aligned}$$

As $(\kappa - \tilde{\kappa}_1 + i\beta)^{-1} \leftrightarrow -2\pi i e^{-i\tilde{\kappa}_1 t - \beta t} \chi(t)$, $\chi(t)$ — being Heaviside's function, so

$$A_{0,2}(t) = -\beta e^{i \arg D} \int\limits_{-\infty}^{t} F_0(t) e^{-i\tilde{\kappa}_1 (t-\tau) - \beta(t-\tau)} d\tau.$$

With $t > 2T$, the part $A_{0,2}(t) = const(\tilde{\kappa}, \alpha, \tilde{\kappa}_1, \beta)e^{-i\tilde{\kappa}_1 t - \beta t}$ completely describes the tail of the pulse $A_0(t)$: the envelope level; the weak attenuation in time ($\beta \ll 1$); the change of high- frequency filling etc. On the change of high-frequency filling it is possible to estimate the value of the deviation of the pulse $F_0(t)$ carrier frequency from the real part of the complex eigen frequency $\overline{\kappa}$. In the considered case (See the fragment with $\overline{\arg} A_0(t)$) the deviation equals to $\tilde{\kappa} - \tilde{\kappa}_1 \approx -10^{-3}$. Up to a certain time, in the interval $0 < t < 2T$, the part $A_{0,2}(t)$ is a background one, the major part $A_0(t)$ of the pulse is determined by the component $A_{0,1}(t)$, which differs from the excitation pulse $F_0(t)$ only by presence of a constant complex factor. With alignment of the levels $A_{0,1}(t)$ and $A_{0,2}(t)$, their contribution in $A_0(t)$ is also partially compensated, for the clear reasons in this moment the phase pulse envelope sharply changes.

The response of the grating to excitation by a narrow band signal is predetermined by the dynamics of the elements of its spectral set Ω_κ. Any of changes of the signal envelope $f_0(\kappa)$ results in easy foreseeing changes in pulses $A_0(t)$ and $B_0(t)$. The schema of analytical treatment is the same, it is only necessary to take into account the changes of the excitation pulse $F_0(t) \leftrightarrow f_0(\kappa)$. In such a manner, there was given (even before numerical analyses) a qualitative study of the pulses $B_0(t)$, the amplitude envelopes of which are presented in Fig. 6, the right row of fragments. In the left line of fragments, here, there are $|b_0(\kappa)|$ (the thin solid line) and $|f_0(\kappa)|$ (the dot line and the thick solid one are the windows completing each other up to the standard bell-shaped form) plotted. The pulses $B_0(t)$ produced by the corresponding incident ones are plotted by the same lines in the right line of fragments. Besides, here there are given an initial pulse (dash line) and the pulse $B_0(t)$ produced by it (thin continuous line) with the standard form (4) of a "window".

4. Deformation of a narrow band pulse, which spectrum is concentrated in the area of a combined resonance on H_{01}- and H_{02}-waves, is, in general terms, the same as in the cases considered in Item 3 (compare Fig. 5 and Fig. 7). Its analytical description gives a single pole (with a pole in a point $\overline{\kappa}$ being an eigen frequency of the H_{02n} oscillation) representation as well, as the second pole (a complex eigen frequency of H_{01n}-eigen mode) is located far from the real axis (See [1], chapter 2), and it does not need to be considered when the window $f_0(\kappa)$ is reasonably narrow, The behavior of tails of the pulses $A_0(t)$ and $B_0(t)$ (See Fig. 7) allows to assert that in this case the amplitude center $F_0(t)$ (the carrying frequency $\tilde{\kappa}$) coincides with $\tilde{\kappa}_1$, and the eigen frequency $\overline{\kappa} = \tilde{\kappa}_1 - i\beta$ has approached practically right up to the real axis of κ. It hardly can be expected that, with particular

values $\theta, \Phi, \varepsilon, \delta$ the spectral domain of the narrow band pulse $F_0(t)$ could "cover" the purely real ($\beta = 0$) eigen frequency of the H_{02n} mode. But if it takes place, then the body of the pulses $A_0(t)$ and $B_0(t)$ repeat (with decrease in each maximum) the pulse $F_0(t)$, the amplitude envelope of the tail passes parallel to the t axis, whereas its high-frequency filling will be determined by the real eigen frequency $\overline{\kappa}$, i.e., the effect of trapping of a part of the pulse energy in the structure near-field, which is to be analytically described further is realized. Let us notice that the relative levels of the main and the tail parts of the pulses $A_0(t)$ and $B_0(t)$ both in this situation and in the situations illustrated with Figures 5–7 can vary over rather wide limits. The determining factors here are the values of the complex constants C and D, which are linearly connected to the Laurent series coefficients of the diffraction characteristics $a_0(\kappa)$ and $b_0(\kappa)$ in small vicinities of points $\overline{\kappa}$ of the spectrum (See [1], Eq. (5.17)).

5. BROAD BAND PULSES SCATTERING

1. In the investigation of deformations of broad band pulses it is necessary to proceed from the space-time fields formed by the grating in the field of non stationary waves $U(g;t) = E_x$, that is the solution of initial boundary value problem

$$\left[-\varepsilon\frac{\partial^2}{\partial t^2} + \frac{\partial^2}{\partial z^2} + \frac{\partial^2}{\partial y^2}\right] U = F(g;t); \quad t > 0, \ g = \{y, z\} \in R; \tag{10}$$

$$U\left\{\frac{\partial U}{\partial y}\right\}(2\pi, z; t) = e^{i2\pi\Phi} U\left\{\frac{\partial U}{\partial y}\right\}(0, z; t);$$

$$U\Big|_{g\in S} = 0, \quad t > 0; \tag{11}$$

$$U(g, 0) = \varphi(g); \quad \frac{\partial}{\partial t} U(g;t)\Big|_{t=0} = \Psi(g) \tag{12}$$

Here same as in problem (1)–(3) Φ — is a real parameter of Floquet channel $R = R = \{g \in Q : 0 \le y \le 2\pi\}$, but in difference with frequency domain, functions $f(U, F, \cdots)$ are to be considered as Fourier images of functions f_{true} describing physically implemented fields and sources [6]:

$$f_{tru}(y, z; t) = \int_{-\infty}^{+\infty} \tilde{f}(z, t; \Phi) e^{i\Phi y} dy$$

$$= \int_{-0.5}^{0.5} \left[\sum_{n=-\infty}^{\infty} \tilde{f}(z,t;n+\Phi) e^{i(n+\Phi)y} \right] d\Phi$$

$$= \int_{-0.5}^{0.5} f(y,z,t;\Phi) d\Phi$$

With certain requirements for $F(g,t)$ φ, Ψ [9] problem (10)–(12) is uniquely solvable in respect to $U(g;t)$ in Sobolev space. $W_2^1(R^T), R^T = R \times (0,T), T < \infty$.

2. It is known, that the spectrum of compact resonators (analogue of discrete spectral set $\{\overline{\kappa}_n\} = \Omega_k$) is free from real eigen frequencies in physical domain of frequency parameter. The presence in the spectrum of gratings such elements of $\overline{\kappa}$ has to be considered as a rule but not as an exception [1]. The reason is in the ability of compensating routine to participate efficiently in the process of forming fields of eigen modes. Inputs of different partial components of eigen field into domains $|z| < 2\pi\delta$ into propagating harmonics in radiation field (see representation (2), when $\tilde{U}^i \equiv 0$) may be summering with opposite phase and compensate each other, closing in fact formally open (their number is always finite) for radiation channels.

The presence of real eigen frequencies $\{\overline{\kappa}_n\}$, the possibility of their closing in the complex space metric K (the natural domain of analytical continuation of the problem (1)–(3) over complex parameter κ) while geometrical and media parameters varying, and the structure of K itself, (infinitely folded Riemann surface with branching points $\tilde{\kappa} \notin \{\kappa_n : \Gamma_n(\kappa_n) = 0\}$) define many of peculiarities in time-space electromagnetic field transformations. We shall illustrate this by the example that is valid for rather wide class of periodic gratings. This class includes gratings of following features: arbitrary shaped boundaries S and S_1, piece wise smooth functions $\varepsilon(g) : \varepsilon(y+2\pi, z) = \varepsilon(y)$, $\varepsilon(y, |z| > 2\pi\delta) \equiv 1$. And, first of all we would remind [1], that resolvent operator-function of the problem (1)–(3) and $\tilde{U}(g;\kappa)$, Green's function $\tilde{G}(g, g_0; \kappa)$ of the grating in the field of point quasi periodic souses, amplitudes $a_n(\kappa)$ and $b_n(\kappa)$ are meromorphic functions of κ within the local in K variables. The poles of these functions are the points $\{\overline{\kappa}_n\} = \Omega_\kappa$, their residues in the poles define corresponding characteristics of eigen modes of periodic structure.

Supposing that there is no accumulating point for elements $\{\overline{\kappa}_n\}$ at the periphery of Reκ axis of the first physical sheet of surface K and applying conventional technique of Laplace transform to problem (10)–(12) with $F(g;t) = f(g)e^{(-i\tilde{\kappa}t)}$, $\mathrm{Im}(\tilde{\kappa}) = 0$, supp$f(g) \in R_\delta = \{g \in$

$R : |z| \le 2\pi\delta\}$ and $\varphi(g) = \Psi(g) \equiv 0$, we arrive for $t \to \infty$:

$$\begin{aligned} U(g;t) \;=\; & \sum_n \int_R \operatorname*{Res}_{\kappa\in\{\overline{\kappa}_n:\mathrm{Im}\overline{\kappa}_n=0\}} \left[\tilde{G}(g,g_0;\kappa)\frac{f(g_0)}{\kappa-\tilde{\kappa}}e^{(-i\kappa t)}\right] dg_0 \\ & + \sum_n \int_R \operatorname*{Res}_{\kappa\in\{\overline{\kappa}_n:-\beta<\mathrm{Im}\overline{\kappa}_n<0\}} \left[\tilde{G}(g,g_0;\kappa)\frac{f(g_0)}{\kappa-\tilde{\kappa}}e^{(-i\kappa t)}\right] dg_0 \\ & + \eta\left[\int_R \tilde{G}(g,g_0;\tilde{\kappa})f(g_0)dg_0\right] e^{(-i\tilde{\kappa}t)} + P_\beta(g,t); \quad g \in R_a \end{aligned} \tag{13}$$

Here: $R_a = \{g \in R : |z| < 2\pi a\}$, $a \ll t$; $\overline{\kappa}_n$ are real and complex poles of Green's function $\tilde{G}(g,g_0;\kappa)$ which are located on the first sheet of the K surface above line $\mathrm{Im}\kappa = -\beta$, $\beta > 0$. According to assumptions made, common number poles is finite. Value η is equal to zero if $\tilde{\kappa} \in \{\overline{\kappa}_n\}$ otherwise it is equal to one. The input of the function $P_\beta(g;t)$ over the norm W_2^1 is estimated as follows: for any of finite a and β there is such T that for $t > T$ the relation $\|P(g,t)\| = o(I)$ is valid if only $\tilde{\kappa} \notin \{\kappa_n\}$.

Consider more thoroughly the solution of non-stationary problem $U(g;t)$, $g \in R_a$, $t \to \infty$. Let the spectrum of open periodic resonator does not contain real eigen frequencies on the first sheet of $K(\{\overline{\kappa}_n : \mathrm{Im}\overline{\kappa}_n = 0\} \neq \emptyset)$ and excitation frequency does not coincide with any of branching points ($\tilde{\kappa} \notin \{\kappa_n\}$). Then

$$U(g;t) = \tilde{U}(g;\tilde{\kappa})e^{(-i\tilde{\kappa}t)} + O(t^{-1}). \tag{14}$$

Where $\tilde{U}(g;\tilde{\kappa})$ is the solution of diffraction problem (1)–(3) with quasi periodic function $f(g)$ in right hand side of equation (1) and $\tilde{U}^i = 0$. From (14) follows that for sufficiently large t the field, scattered by grating at any finite distance from this grating comes onto harmonic regime and the principle of limit amplitude is implemented.

The most interesting appears to be a situation when the real spectrum of the open periodic resonator is not empty ($\{\overline{x}_n : \mathrm{Im}\overline{x}_n = 0\} \neq \emptyset$). Since only the simple poles of function $\tilde{G}(g,g_0,x)$, are connected with such elements of the spectral set Ω_κ [1], it is derived

$$\begin{aligned} U(g;t) \;=\; & \tilde{U}(g;\tilde{\kappa})e^{(-i\tilde{\kappa}t)} + \sum_{n:\mathrm{Im}\overline{\kappa}_n=0} \frac{A_n(f)}{\overline{\kappa}_n-\tilde{\kappa}}\tilde{U}_n(g;\overline{\kappa}_n)e^{(-i\overline{\kappa}_n t)} \\ & + \begin{cases} O(t^{-1}), & \tilde{\kappa} \notin \{\kappa_n\} \\ O(1), & \tilde{\kappa} \in \{\kappa_n\} \end{cases} \end{aligned} \tag{15}$$

in the case when the frequency $\tilde{\kappa}$ is not eigen one for the given structure, and the relation

$$U(g;t) = \sum_{n\neq m} \frac{A_n(f)}{\overline{\kappa}_n - \tilde{\kappa}} \tilde{U}_n(g;\overline{\kappa}_n) e^{(-i\overline{\kappa}_n t)} - iA_m(f) t \tilde{U}_m(g,\overline{\kappa}_m) \exp(-i\tilde{\kappa}t)$$
$$+ \left\{ \int\limits_R \frac{\partial}{\partial\kappa} \left[\tilde{G}(g,g_0;\kappa)(\kappa - \overline{\kappa}_m) \right]_{\kappa=\overline{\kappa}_m} f(g_0) dg_0 \right\} e^{(-i\tilde{\kappa}t)}$$
$$+ O(t^{-1}); \quad g \in R_a \tag{16}$$

is valid for $\tilde{\kappa} = \overline{\kappa}_m \in \{\overline{\kappa}_n : \mathrm{Im}\overline{\kappa}_n = 0\}$. Here: $A_n(f)$ are amplitudes, depending on $f(g)$, geometrical and media parameters of gratings; $\tilde{U}_n(g;\overline{\kappa}_n)$ are eigen functions corresponding to real eigen frequency $\overline{\kappa}_n$, and

$$A_n(f)\tilde{U}_n(g;\kappa_n) = \int\limits_R \mathrm{Res}\tilde{G}(g,g_0,\overline{x}_n) f(g_0) dg_0 \equiv 0.$$

At the excitation frequency $\tilde{\kappa}$ close to that of the eigen frequency, $\overline{\kappa}_m \in \{\overline{\kappa}_n : \mathrm{Im}\overline{\kappa}_n = 0\}$, but not coincident with it, the principal term in the expansion of Eq. (15) is determined by the expression:

$$R(g;t) = \frac{A_m(f)}{\overline{\kappa}_m - \tilde{\kappa}} \tilde{U}_m(g;\overline{\kappa}_m)(e^{(-i\overline{\kappa}_m t)} - e^{(-i\tilde{\kappa}t)}).$$

It dominates in the field formed by the grating not for the whole time. Approaching the excitation frequency close to that of eigen frequency of the structure results in occurrence of beats with $\min|R(g;t)| = 0$ when $(\overline{\kappa}_m - \tilde{\kappa})t = 2\pi j$, $j = 0, \pm 1 \ldots$, and with $\max|R(g;t)|$ when $(\overline{\kappa}_m - \tilde{\kappa})t = (2j+1)\pi$. At the time moment when the maximal value of $|R(g;t)|$ is reached, the scattered field, is completely determined by the eigen field existing at the $\kappa = \overline{\kappa}_m$ frequency. With t increase the relation between the energies of fields, which is determined by the main part and the background one of $U(g;t)$ remains practically constant (on the order of t). Energy of a continuously operating source is rescattered by the grating into Fraunghofer zone $|z| \gg 1$.

Quite a different situation develops when $\tilde{\kappa} = \overline{\kappa}_m$. In this case, from Eq. (16) it is obtained

$$R(g;t) = -iA_m(f) t \tilde{U}_m(g;\overline{\kappa}_m) e^{(-i\tilde{\kappa}t)} \quad g \in R_a$$

This result means that the energy is stored in the near field of the grating.

It would be possible to comment on some other examples of non-standard behavior of the fields formed by open periodic resonator. But it is already clear that the only source of reliable information about field's evolution within finite interval of time can be the computing experiment; the experiment, relying on rigorous models and corresponding efficient algorithms. Such models and algorithms, have, which is very important, to differentiate the contribution of each of various components into the total resulting field.

3. The drastic expansion of the spectral domain of the signals requires adequate changes in the methods and techniques of their numerical treatment, since use of Fourier transform becomes problematic because of presence of high and very high frequencies at the spectrum of the signals, while the individual influence of "natural resonances", which was taken into account earlier in the frameworks of the well-proved local representations for $\tilde{U}(g;\kappa)$ in small vicinities of points $\overline{\kappa} \in \Omega_\kappa$ gives way to collective influence of the greater part of the elements making up the set Ω_κ To isolate the contribution of any group or one of the elements and thus to understand the physics of what is going on within a rather small interval, (i.e., an analytical analysis of transients) is a very complicated problem, requiring significant efforts aimed at realization of problem-oriented computational experiments and development of a special technique of both processing and the analysis of their results. Here we only demonstrate results (See Figs. 8–10) and our readiness to solve this problem, namely, the existence of operating algorithms making possible to visualize the transient fields in a near zone of gratings excited by broad band pulses.

In Figs. 8, 9 it is a pulse

$$U^i(g;t) = f(t+z)e^{i\Phi y} - \frac{\Phi}{2}e^{i\Phi y}\int\limits_{z-t}^{z+t} f(z_0)(t-z+z_0)\frac{J_1(\Phi\sqrt{t^2-(z-z_0)^2})}{\sqrt{t^2-(z-z_0)^2}}dz_0$$

with $f(t) = e^{-(t-T)^2/\alpha^2}e^{-i\tilde{\kappa}(t-T)}$, $\Phi = 0.1$, $T = 7.8$, $\tilde{\kappa} = 0.76066$, and $\alpha = 1$.

Its amplitude envelope in a plane $z = 2\pi\delta$ is plotted in Fig. 8, a by dash line; the value of δ, as well as the values of the other structure parameters (the grating from beams with a dielectric filling of the slots) are kept without changes. The fields $U(g,t)$ are described by the solutions of the initial-boundary problem (10)–(12), where in this case $F(g;t) \equiv 0$ and $U(g;0) = U^i(g;0)$, while in case of Fig. 10, $\varphi(g) = \psi(g) \equiv 0$. The pulses $A_0(t)$ and $B_0(t)$ as well as before, are principal partial components of reflected $U^s(g;t) = U(g;t) - U^i(g;t)$ and transmitted $U(g,t)$ fields in the planes of $z = 2\pi\delta$ and $z = -2\pi\delta$, i.e., they are zero Fourier- expansion coefficients of corresponding

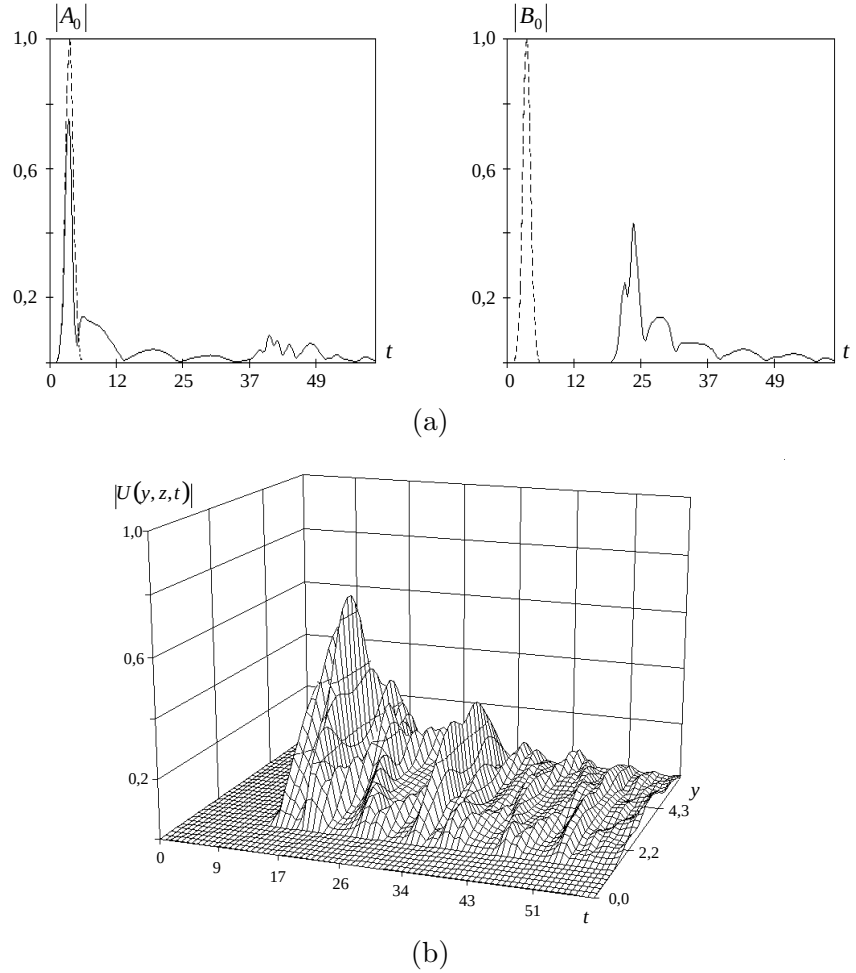

Figure 8. Grating in the field of a wide band pulse: a) absolute values of $U^i(t)$ envelopes (dashed line) and $A_0(t)$, $B_0(t)$ (Solid line); b) field $U(y, z, t)$ in the plane of structure symmetry $z = 0$.

functions with respect to the system of functions $\{e^{(i\Phi_n y)}\}_n$ complete on the interval $0 \leq y \leq 2\pi$.

The carrying frequency $\tilde{\kappa}$ of the pulse $U^i(g, t)$ coincides with the real part of eigen frequencies $\overline{\kappa}$ of the H_{02n} eigen mode (hybrid), practically approaching the real κ axis (See Item 4 of Section 4). But this circumstance, in the considered time intervals, has no appreciable effect on the space-time field configuration, i.e., the results practically

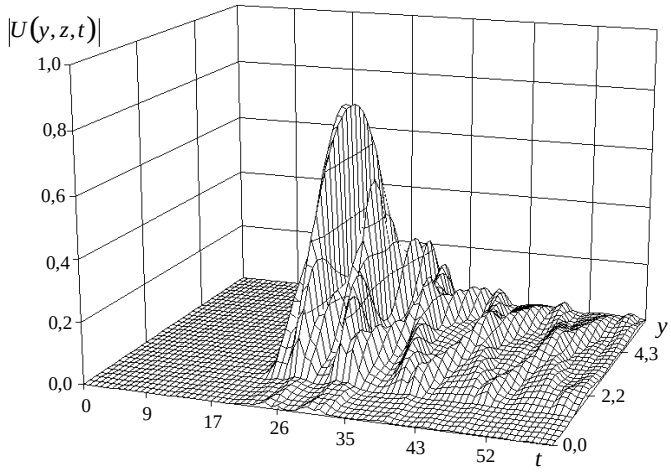

(a)

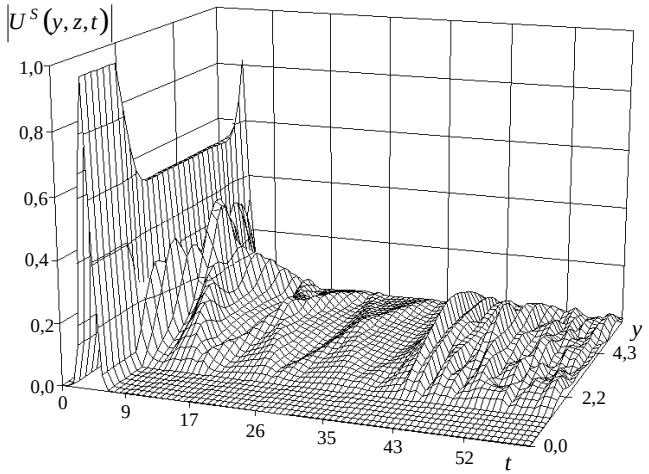

(b)

Figure 9. Grating in the field of super wide band pulse: a) field $U(y, Z, t)$ in the plane $z = -2\pi\delta - \gamma$, $0 < \gamma \ll 1$; b) reflected field $U^S(y, z, t) = U(y, z, t) - U^i(y, z, t)$ in the plane $z = 2\pi\delta$.

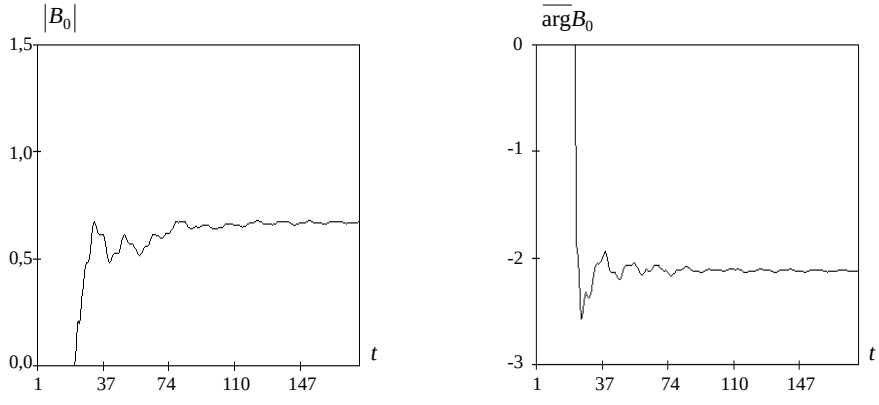

(a)

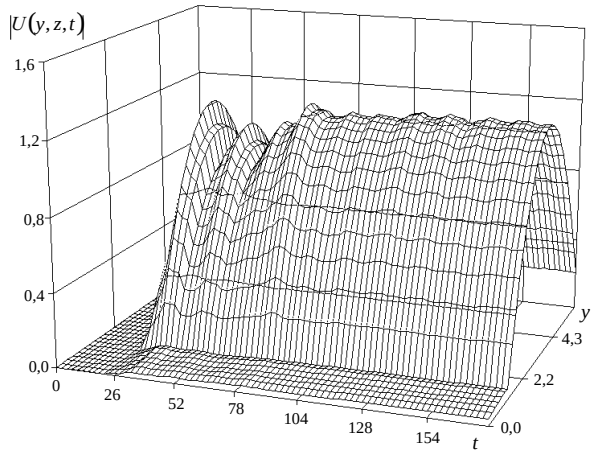

(b)

Figure 10. Grating in the field of constantly operating source: a) the principal partial component in the transmission domain; b) field $U(y, z, t)$ in the plane $z = -2\pi\delta - \gamma$, $0 < \gamma \ll 1$.

repeating those shown in Figs. 8, 9 are obtained as well both for the values $\tilde{\kappa} = 0$; $\tilde{\kappa} = 0.499$ (H_{01n} pure mode resonance) and $\tilde{\kappa} = 0.69182$ (a pure resonance of H_{02n}-mode). The over wide spectral range of the excitation pulse erases the distinctions connected to relatively small shifting of the amplitude center. These distinctions will most likely show themselves at large time t values and on large distances from the structure aperture planes $|z| = 2\pi\delta$.

4. The result shown in Fig. 10, is analytically described by the issue 2 of this Section: a constantly operating source

$$F(g;t)=\left\{\begin{array}{rl} 10(i\tilde{\kappa})^2e^{-i\tilde{\kappa}t}e^{i\Phi y}, & |z-7.8|\le 0.1 \\ 0, & |z-7.8|>0.1 \end{array}\right. ;\ \tilde{\kappa}=0.76066,\ \Phi=0.1$$

generates a non-stationary field, in which a harmonic operation mode with frequency $\kappa=\tilde{\kappa}$ is established as time elapses. Ultimate quick fixing of such mode is promoted by the fact that $\tilde{\kappa}$ coincides with the real part of eigen frequency of H_{02n} mode, whereas the imaginary part of this eigen frequency is very small. Competing harmonic components are absent (or they quickly damp), as the grating does not support eigen fields with real eigen frequencies (the first wave connecting the domains of reflection with transmission ones occurs only with $\kappa>0.317$, i.e., in the area of $\kappa>\Phi$, where the channel of radiation of energy in free space is already open), and the other complex eigen frequencies are located much further away from the real axis in the complex variable κ plane.

On closing the question, we would give one more illustration of the super wide band pulse distortion by reflecting grating. Fig. 11 shows scattering characteristics if sin-shaped reflecting grating $z=\pi\beta(\sin y-1)$ (Fig. 11b) exited by Gauss type pulse $U^i(g;t)=e^{-(t+z-T^2)/\alpha^2}$, $T=0.6$ and $\alpha=0.2$. Pulses $A_n(t)$ are the partial components of the Fourier expansion of $U^S(g;t)=U(g;t)-U^i(g;t)$ over the function system $\{e^{iny}\}_n$ in the plane $z=0$. The structure's response may be foreseen: the reflecting abilities of elements of surface operating in specula regime are dominating; there is clear correlation between the field distribution $|U^S(y,0;t)|$ and the profile of smooth grating; time-space focusing of the field by the cavity of grating of deep profile occurs.

6. PULSE PROPAGATION IN REGULAR SECTIONS OF FLOQUET CHANNELS

1. The pulse deformation is caused not only by the scattering by resonance in homogeneities of the Floquet channel but it also occurs in the process of free propagation over finite-length segments of the "wave guiding line" of the kind. In this case, the decisive role is played by some specific factors which must be given a detailed account in designing functional units whose operation is controlled by the signal particular shape and duration. In our consideration, we proceed from the methodology, which gains popularity among many authors concerning with the pulse propagation in homogeneous (dispersive and

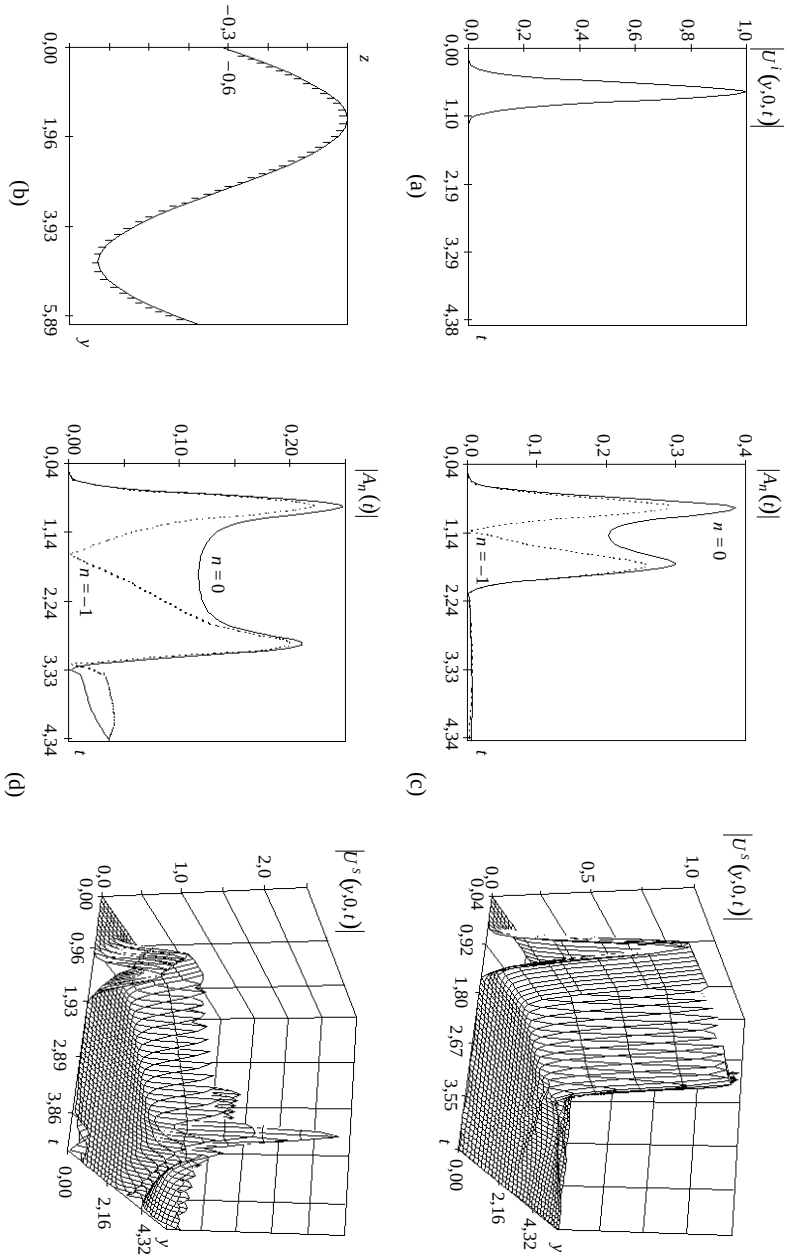

Figure 11. Electromagnetic characteristics of sine shaped gratings: $z = \beta\pi(\sin y - 1)$; (c) $\beta = 0.1$; (d) $\beta = 0.2$.

absorbing) media and circuits. A most concentrated description of the results on the subject can be found in [8, 10, 11]. Assume that the field

$$U^s(g;t) = \sum_{n=-\infty}^{\infty} w_n(z,t)e^{i\Phi_n y}, \quad z \geq 0$$

is formed by a grating and defined by the values

$$w_n(0,t) = A_n(t) = \int_{-\infty}^{\infty} a_n(\kappa)e^{-i\kappa t}d\kappa \quad \leftrightarrow a_n(\kappa)$$

of elements $w_n(z,t)$ of evolutionary basis [5, 6] given in cross section of the channel R in plane $z = 0$. The $U^s(g;t)$ evolution due to the nonsine wave propagation toward large z may be modeled both in frequency domain terms

$$w_n(z,t) = \int_{-\infty}^{\infty} a_n(\kappa)e^{i(\Gamma_n z - \kappa t)}d\kappa \leftrightarrow a_n(\kappa)e^{i\Gamma_n z} \tag{17}$$

and directly in the time-space domain

$$w_n(z,t) = w_n(0,t-z) - \Phi_n z \int_0^{t-z} w_n(0,\tau)\frac{J_1(\Phi_n\sqrt{(t-\tau)^2 - z^2})}{\sqrt{(t-\tau)^2 - z^2}}d\tau. \tag{18}$$

The first representation is evident, and it serves the basis for deriving the second one when referring to the properties of the Fourier transform convolution (*):

$$\begin{aligned} w_n(z,t) &= \int_{-\infty}^{\infty} a_n(\kappa)e^{i(\sqrt{\kappa^2-\Phi_n^2}z - \kappa t)}d\kappa \\ &= \left(\int_{-\infty}^{\infty} a_n(\kappa)e^{-i\kappa t}d\kappa\right) * \left(\int_{-\infty}^{\infty} e^{i\sqrt{\kappa^2-\Phi_n^2}z}e^{-i\kappa t}d\kappa\right) \\ &= w_n(0,t) * \left(\int_{-\infty}^{\infty} e^{i\sqrt{\kappa^2-\Phi_n^2}z}e^{-i\kappa t}d\kappa\right). \end{aligned} \tag{19}$$

Substituting

$$\int_{-\infty}^{\infty} e^{i\sqrt{\kappa^2-\Phi_n^2}z}e^{-i\kappa t}d\kappa = \frac{\partial}{\partial z}\int_{-\infty}^{\infty}\frac{e^{i\sqrt{\kappa^2-\Phi_n^2}z}}{i\sqrt{\kappa^2-\Phi_n^2}}e^{-i\kappa t}d\kappa$$

$$\begin{aligned} &\underset{-i\kappa=p}{=} -2\pi\frac{\partial}{\partial z}\left(\frac{1}{2\pi i}\int\limits_{-i\infty}^{i\infty}\frac{e^{-\sqrt{p^2+\Phi_n^2}z}}{\sqrt{p^2+\Phi_n^2}}e^{pt}dp\right)\\ &= -2\pi\frac{\partial}{\partial z}\left(J_0(\Phi_n\sqrt{t^2-z^2})\chi(t-z)\right)\\ &= 2\pi\left(\delta(t-z)-\Phi_n z\frac{J_1(\Phi_n\sqrt{t^2-z^2})}{\sqrt{t^2-z^2}}\chi(t-z)\right)\end{aligned}$$

into (19) with assuming $w_n(0,t)=0$ at $t<0$ yields (18). Here again $J_m(\cdots)$ is the Bessel function and $\chi(\cdots)$ is the Heaviside function. In the following analysis, subscript n of values w_n, Γ_n, Φ_n is of no concern, so it will be omitted.

Figs. 12–17 plot calculations by formula (17) for narrow band pulses, with functions $a(\kappa)$ chosen as

$$a(\kappa)=e^{-\alpha^2(\kappa-\tilde\kappa)^2}e^{iT\kappa} \quad\leftrightarrow\quad w(0,t)=\frac{\sqrt{\pi}}{\alpha}e^{-\frac{(t-T)^2}{4\alpha^2}}e^{-i\tilde\kappa(t-T)} \tag{20}$$

$$a(\kappa)=e^{\frac{\alpha^2}{(1+4i\beta\alpha^2)}(\kappa-\tilde\kappa)^2}e^{iT\kappa} \quad\leftrightarrow\quad w(0,t)=\frac{\sqrt{\pi(1+4i\beta\alpha^2)}}{\alpha}e^{-\frac{(t-T)^2}{4\alpha^2}} \times e^{-i\tilde\kappa(t-T)}e^{-i\beta(t-T)^2} \tag{21}$$

Function $w(0,t)$ has its maximum at a point T, and the main contribution it receives from the interval $[T-6\alpha, T+6\alpha]$. Off it, $w(0,t)$ values are less than $w(0,T)\cdot 10^{-3}$. The $a(\kappa)$ values with a maximum at a point $\tilde\kappa$ are concentrated in the interval $[\tilde\kappa-3/\alpha, \tilde\kappa+3/\alpha]$. Off it, $a(\kappa)$ values are less than $a(\tilde\kappa)\cdot 10^{-3}$.

For broadband pulses, Figs. 18–20 report calculations of function $w(z,t)$ by formula (18). The time delay T is so chosen that function $w(0,t)$ is assumed to vanish for $t<0$. In all the figures, the distance scale z is established by m according to $z=2\pi m\alpha$.

If a frequency band occupied by pulses with spectral amplitudes (20), (21) does not include a threshold point κ: $\Gamma(\kappa)=0$ of the Floquet channel, function $\Gamma(\kappa)$ in (17) can be substituted, provided α is sufficiently large, by a finite segment of its Laurent series

$$\Gamma(\kappa)=\Gamma(\tilde\kappa)+\Gamma'(\tilde\kappa)(\kappa-\tilde\kappa)+\frac{\Gamma''(\tilde\kappa)}{2}(\kappa-\tilde\kappa)^2+\frac{\Gamma'''(\tilde\kappa)}{6}(\kappa-\tilde\kappa)^3+\cdots.$$

Here Γ', Γ'', and so on are the derivatives of function $\Gamma(\kappa)$ with respect to κ. If $\mathrm{Im}\Gamma(\kappa)=0 (\Gamma'(\tilde\kappa)=\tilde\kappa/\Gamma(\tilde\kappa)>0, \Gamma''(\tilde\kappa)=-\Phi^2/\Gamma^3(\tilde\kappa)<0)$ this substitution hardly affects the exact meaning of the integral in (17) for all z, and one may obtain the closed form expression for $w(z,t)$:

$$
\begin{array}{l}
w(0,t)=\dfrac{\sqrt{\pi}}{\alpha} \qquad \times e^{-\frac{t^2}{4\alpha^2}} \qquad \times e^{-i\tilde{\kappa}t} \\
\qquad \Downarrow 1 \qquad\qquad \Downarrow 2 \qquad\qquad \Downarrow 3 \qquad\qquad \Downarrow 4 \\
w(z,t)=\dfrac{\sqrt{\pi}}{4\sqrt{\alpha^4+\dfrac{z^2\Phi^4}{4\Gamma^6}}}\times e^{-\frac{\left(t-\frac{z\tilde{\kappa}}{\Gamma}\right)^2}{4\left[\alpha^2+\frac{z^2\Phi^4}{4\alpha^2\Gamma^6}\right]}}\times e^{-i\left[\tilde{\kappa}t-\frac{\left(t-\frac{z\tilde{\kappa}}{\Gamma}\right)^2\left(\frac{z\Phi^2}{2\alpha^2\Gamma^3}\right)}{4\left[\alpha^2+\frac{z^2\Phi^4}{4\alpha^2\Gamma^6}\right]}\right]}\times e^{i\left[z\Gamma-\frac{1}{2}\arg\left(\alpha^2+\frac{iz\Phi^2}{2\Gamma^3}\right)\right]}
\end{array}
\tag{22}
$$

$$
\begin{array}{l}
w(0,t)=\dfrac{\sqrt{\pi(1+4i\beta\alpha^2)}}{\alpha} \qquad \times e^{-\frac{t^2}{4\alpha^2}} \qquad \times e^{-i(\tilde{\kappa}t+\beta t^2)} \\
\qquad \Downarrow 1 \qquad\qquad \Downarrow 2 \qquad\qquad \Downarrow 3 \qquad\qquad \Downarrow 4 \\
w(z,t)=\dfrac{\sqrt{\pi(1+4i\beta\alpha^2)}}{\alpha\sqrt[4]{(1+2z\Gamma''\beta)^2+\dfrac{z^2\Gamma''^2}{4\alpha^4}}}\times e^{-\frac{(t-z\Gamma')^2}{4\alpha^2\left[(1+2z\Gamma''\beta)^2+\frac{z^2\Gamma''^2}{4\alpha^4}\right]}}\times e^{-i\left(\tilde{\kappa}t+\frac{(t-z\Gamma')^2\left(4\beta\alpha^2+\frac{\Gamma''z}{2\alpha^2(1+2z\Gamma''\beta)}\right)}{4\left[\alpha^2(1+2z\Gamma''\beta)+\frac{z^2\Gamma''^2}{4\alpha^2(1+2z\Gamma''\beta)}\right]}\right)}\times e^{i\left[z\Gamma-\frac{1}{2}\arg\left(\alpha^2-\frac{i\Gamma''z}{2}+2z\Gamma''\beta\alpha^2\right)\right]}
\end{array}
\tag{23}
$$

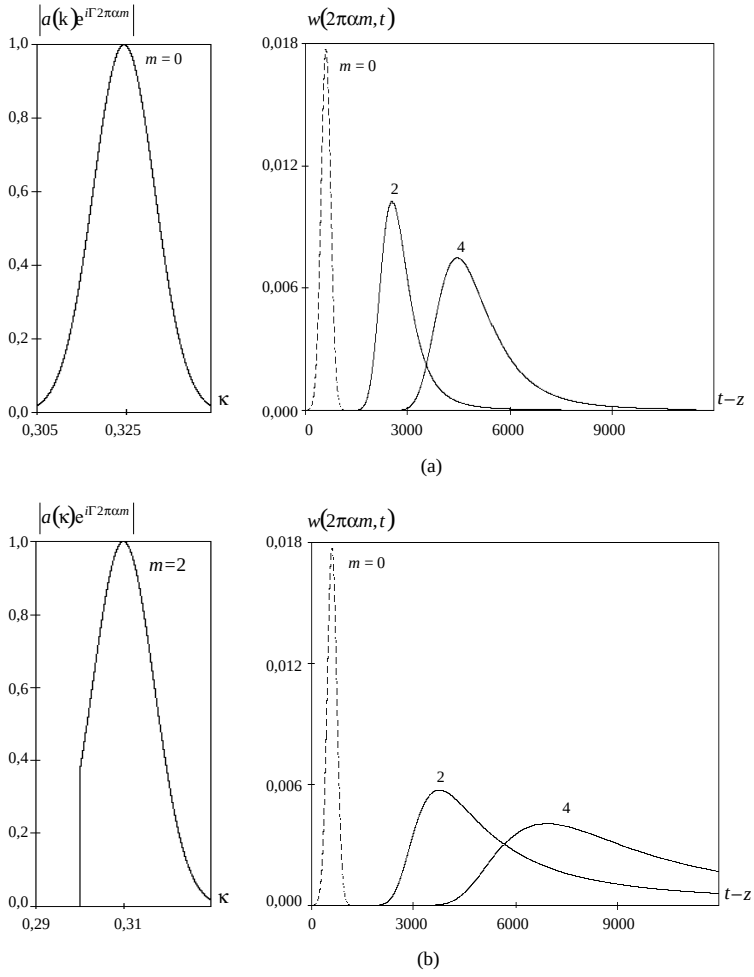

Figure 12. Propagation of narrow band pulse (17), (20) along regular Floquet channel: $\alpha = 100$; $\Phi = 0.3$; $T = 600$. (a) $\tilde{\kappa} = 0.325$; (b) $\tilde{\kappa} = 0.31$.

Here for simplicity's sake, we take $T = 0$ and exclude argument $\kappa = \tilde{\kappa}$ for function $\Gamma(\kappa)$ and its derivatives.

The factors in formulae (22), (23) are so decomposed as to easily estimate the changes arising in the main pulse characteristics while propagating toward large z. A comparison of the two first factors in (22) allows us to reveal a change in the amplitude envelope of the Gaussian pulse with real envelope function when starting from the

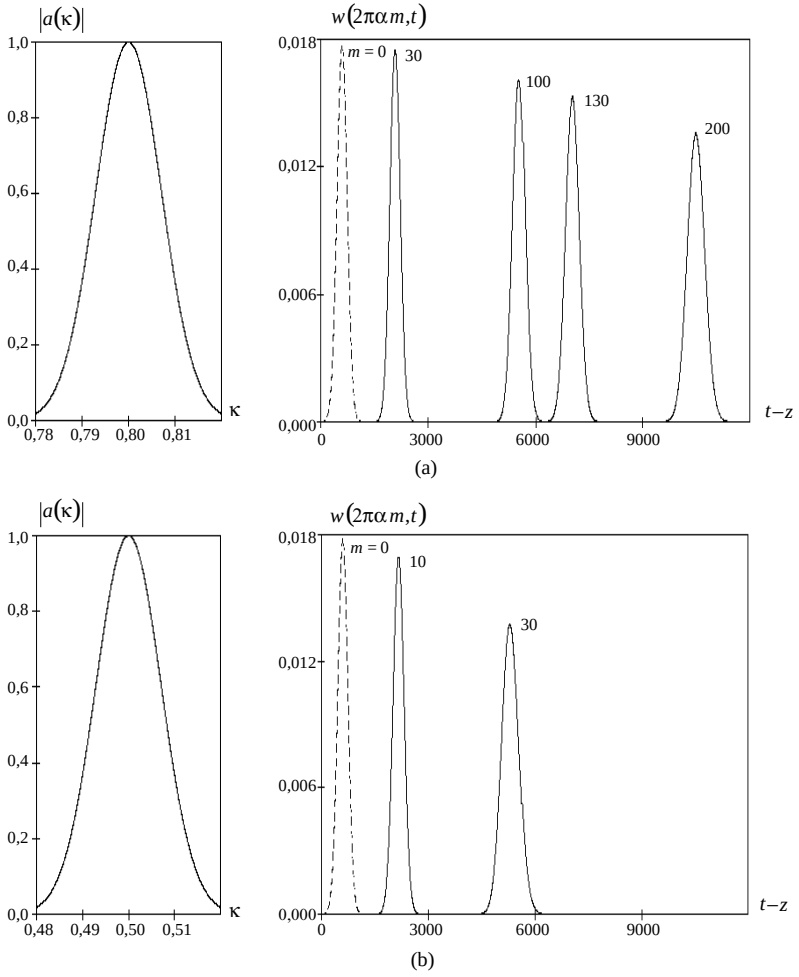

Figure 13. The influence of high frequency filling onto pulse propagation (17), (20): $\alpha = 100$; $\Phi = 0.3$; $T = 600$. (a) $\tilde{\kappa} = 0.8$; (b) $\tilde{\kappa} = 0.5$.

plane $z = 0$. Evidently the pulse shape is unaffected at the same time as the signal duration increases and the amplitude center height goes down as $(1 + 0.25z^2\Phi^4\Gamma^{-6}\alpha^{-4})^{-1/4}$. Besides, the second factor adds information about the average group velocity

$$\nu_{gr} = \Gamma/\tilde{\kappa} = \left(1 - \Phi^2/\tilde{\kappa}^2\right)^{1/2} \leq 1, \tag{24}$$

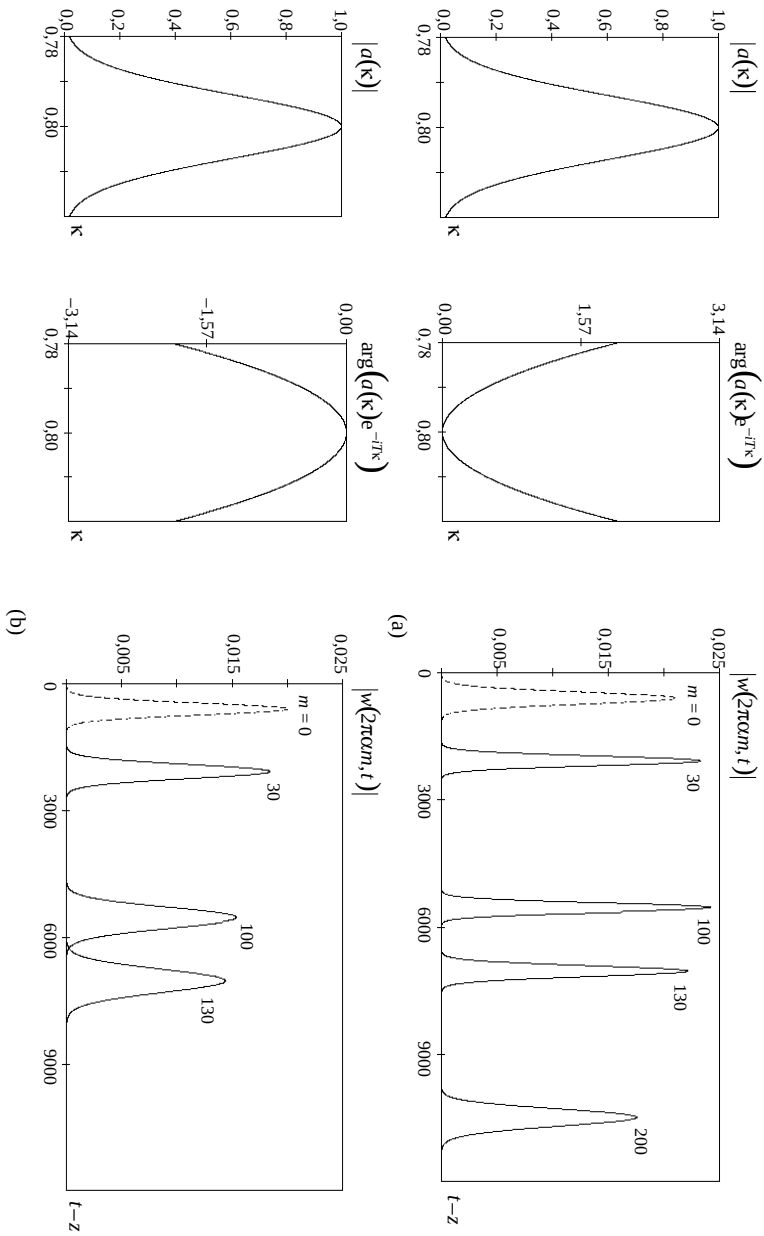

Figure 14. Propagation of narrow band Gaussian pulse (17), (21) with quadratic phase modulation $\alpha = 100$; $\Phi = 0.3$; $T = 600$; $\tilde{\kappa} = 0.8$. (a) $\beta = 1/4\alpha^2$; (b) $\beta = -1/4\alpha^2$.

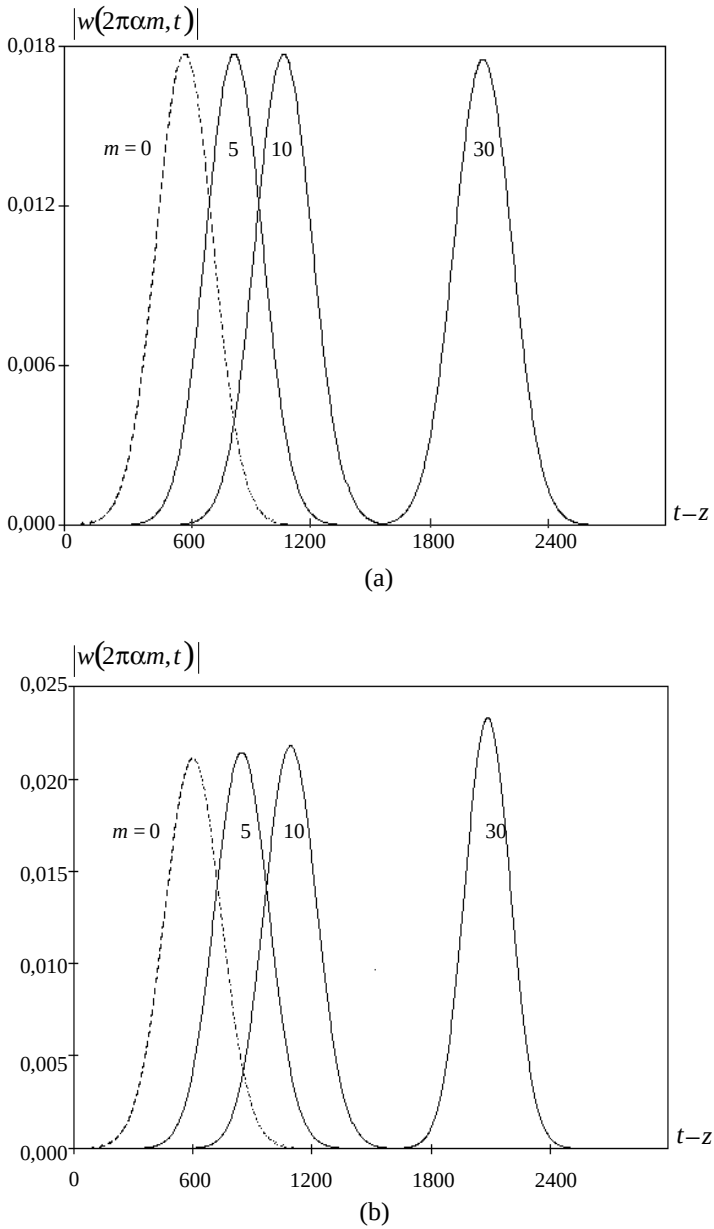

Figure 15. "Near region" of pulse propagation with real envelope (a) and the pulse with quadratic phase modulation ((b) $\beta = l/4\alpha^2$): $\alpha = 100$; $\Phi = 0.3$; $T = 600$; $\tilde{\kappa} = 0.8$.

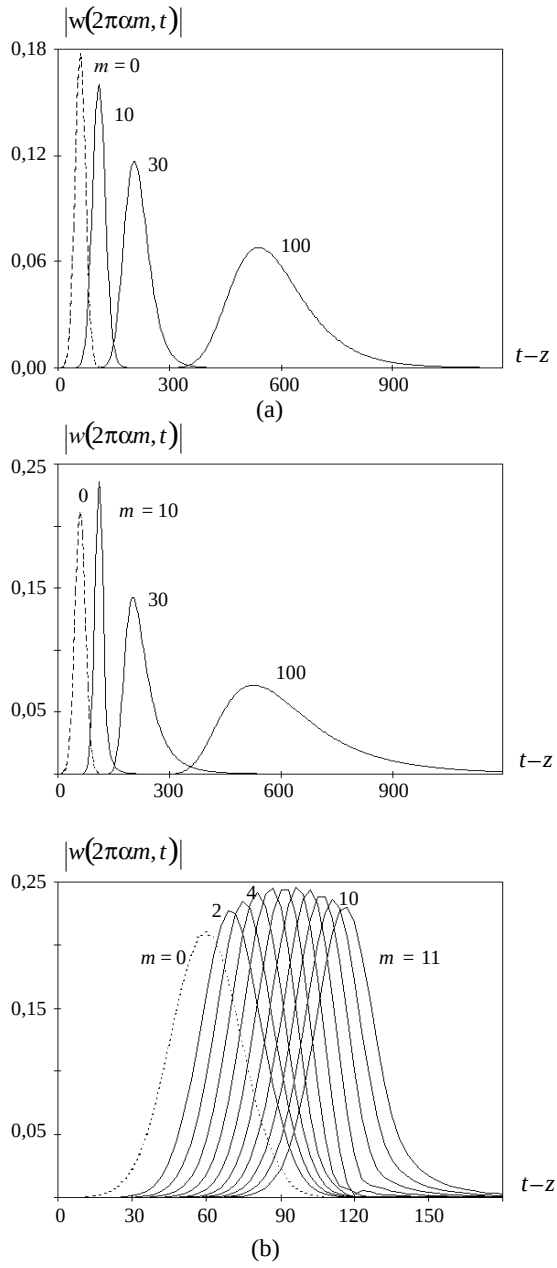

Figure 16. Time-space focusing of the pulse with quadratic phase modulation: $\alpha = 10$; $\Phi = 0.3$; $T = 60$; $\tilde{\kappa} = 0.8$, (a) $\beta = 0$; (b) $\beta = 1/4\alpha^2$.

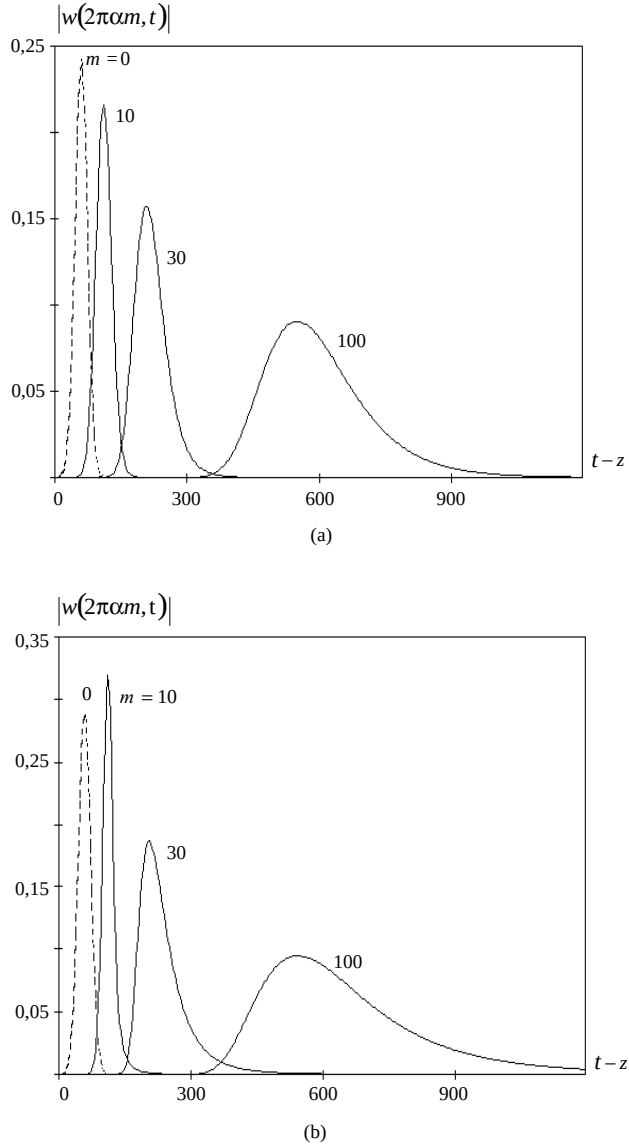

Figure 17. The focusing process of the pulse, resulted from δ-source in the plane $z = 0$: $\alpha = 10$; $\Phi = 0.3$; $T = 60$; $\tilde{\kappa} = 0.8$. (a) $\beta = 0$; (b) $\beta = 1/4\alpha^2$.

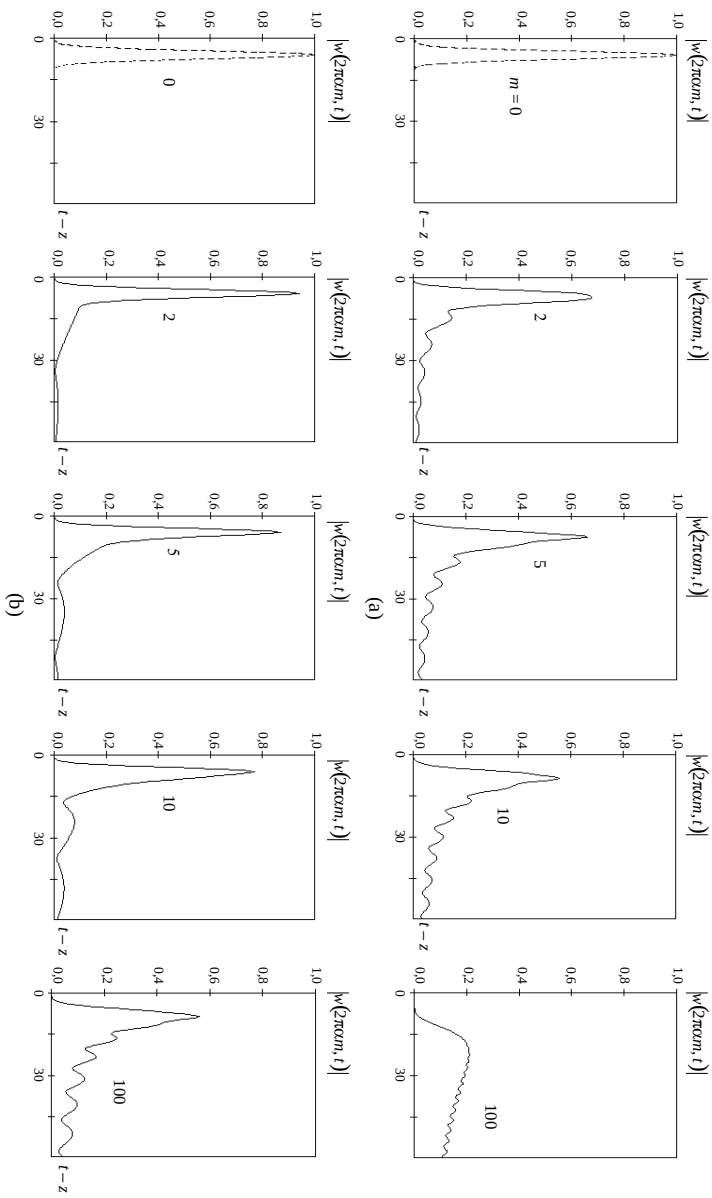

Figure 18. Propagation of the pulse with real envelope function in Floquet channel for different parameters Φ: $w(0,t) = \exp[-(t - T)^2/4\alpha - i\tilde{\kappa}(t - T)]$; $\alpha = 1$; $T = 6$; $\tilde{\kappa} = 0.8$. (a) $\Phi = 0.3$; (b) $\Phi = 0.1$.

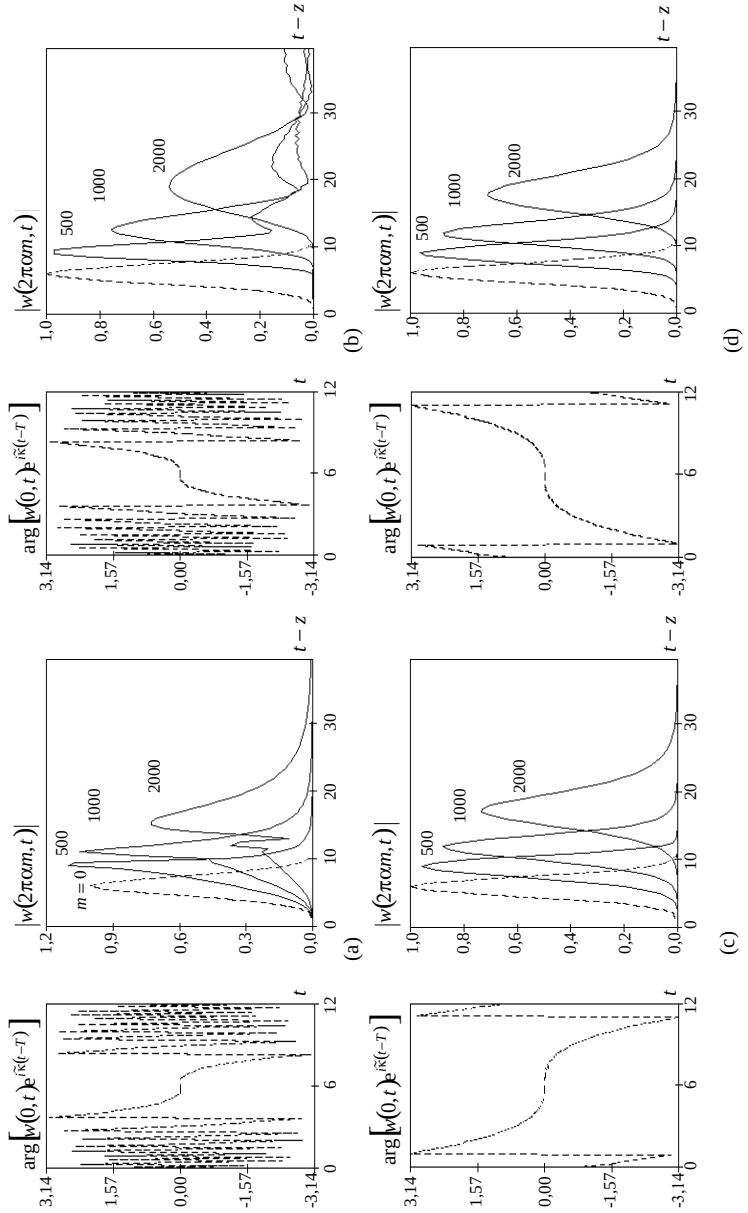

Figure 19. Propagation of the pulse with cubic phase modulation: $w(0,t) = \exp[-(t-T)2/4\alpha^2 - i\tilde{\kappa}(t-T) - i\tilde{\kappa}(t-T)^3]$; $\alpha = 1$; $\Phi = 0.3$; $T = 6$; $\tilde{\kappa} = 7$. (a) $\gamma = 0.25$; (b) $\gamma = -0.25$; (c) $\gamma = 0.025$; (d) $\gamma = -0.025$.

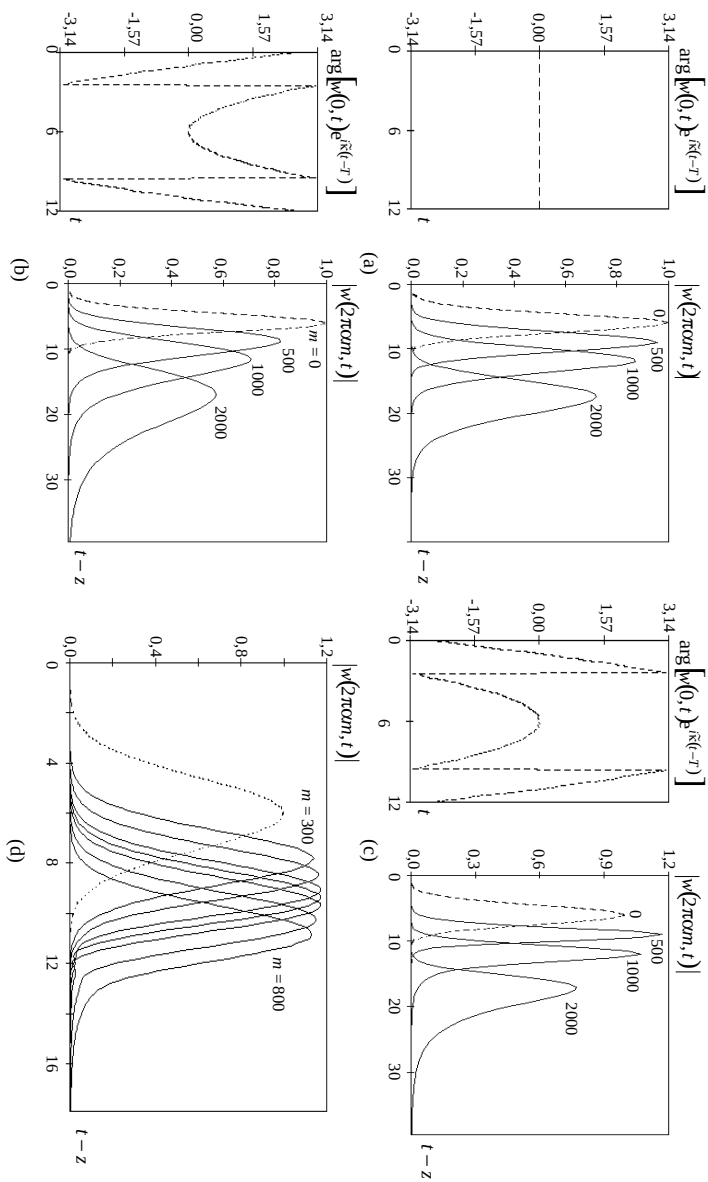

Figure 20. Propagation and focusing of the wide band pulses with quadratic phase modulation: $w(0,t) = \exp[-(t-T)^2/4\alpha^2 - i\tilde{\kappa}(t-T) - i\beta(t-T)^2]$; $\alpha = 1$; $\Phi = 0.3$; $T = 6$; $\tilde{\kappa} = 7$. (a) $\beta = 0$; (b) $\beta = -0.25$; (c) $\beta = 0.25$, results presented in low fragment are calculated for $m = 0$ (dashed line), $m = 300$, 400, 500, 550, 600, 700, 800.

that is velocity of the principal part of the pulse. With same value of parameter Φ of Floquet channel R, the pulses whose central frequency $\tilde{\kappa}$ is higher travel faster. With the same high-frequency content, different partial components of the field $U^s(g;t)$ (components with numbers $n_1 \neq n_2$) exhibit equal group velocities only when their "propagation constants" Γ_{n_1} $(\tilde{\kappa})$ and $\Gamma_{n_2}(\tilde{\kappa})$ coincide. Called auto collimation, this frequency- domain mode with coinciding Γ is used in the synthesis of planar mirrors intended to concentrate completely the scattered field energy in the harmonics traveling toward the incident wave (the effect of total non-specula return — see [1, 2, 7]). A controllable stratification in time of partial components of the scattered field on a basis of different group velocities of particular pulses open up the new opportunities for efficient application of the selective properties of gratings.

The third factor runs the dynamics of varying the high-frequency content and the phase (quadratic) modulation induced in the propagation process. The fourth, supplementary factor arises due to the spatial reconstruction of the phase envelope of the signal. It should be noticed that at $\Phi = 0$ none of the main characteristics of the pulse traveling now at the speed of light is affected.

Our theoretical predictions agree well with numerical experiments (see, e.g., Figs. 12a and 13: a difference in the group. velocities among the pulses with different high- frequency content is clearly recognized; the pulses with higher $\tilde{\kappa}$ run to great distance keeping the main characteristics almost unaffected, etc.). Besides, the numerical experiment allows investigations to be made of situations whose analysis cannot be correct in the frames of the used scheme. Thus a signal's non analyticity (even weak) in the frequency domain (see Fig. 12b: a threshold point $\kappa : \Gamma(\kappa) = 0$ falls in the frequency band occupied by the pulse) causes, even weak, a dramatic change in the energy spectrum (left plot), the amplitude center is quickly spread out, a long-lived tail is developed and comes into a competition with the principal part.

3. For the Gaussian pulse with quadratic phase modulation starting from the plane $z = 0$, the analysis by formulae (23) at $\beta < 0$ extracts no regularities to be qualitatively different from those already mentioned (see, e.g., Fig. 14b).

At $\beta > 0$, it is seen that function $f(z) = (1 + 2z\Gamma''\beta)^2 + z^2\Gamma''^2/(4\alpha^4)$ defining qualitative parameters of the amplitude envelope rises with z non monotonically: at first it falls at the point $z_f = 8\alpha^4\beta\Gamma^3[(1 + 16\alpha^4\beta^2)\Phi^2]^{-1}$, $\Phi \neq 0$ down to the value $f(z_f) = (1 + 16\alpha^4\beta^2)^{-1}$, and only then it comes to a stage of continuous increase. Point z_f is a space one, which is passed through at a most compression

of the principal part of the pulse. In the other words, this is a maximum focusing point of the nonsine wave. The attainable compression is given by the value $f(z_f)$ which rises with α and β, no matter which is the Floquet channel parameter ($\Phi \neq 0$) and high-frequency filling $\tilde{\kappa}$. The group velocity of the pulse with quadratic phase modulation remains the same, as it is for the pulse with real envelope (see, e.g., Figs. 14–16). For the latter, a change of the phase envelope with the pulse traveling (see (22)) is caused, among other things, by the induced quadratic (in time) modulation which however is such that does not produce a subsequent focusing of the pulse (a parameter which fulfils the role of β is negative for all z). The foreseen or already happened focusing is readily detected by the calculations of the pulse characteristics when made for different propagation distances (see Figs. 14, 15). A detailed consideration is given to this phenomenon in Fig. 16b (lower plot).

A change in the amplitude envelope of the starting signal produces no effect on its self-focusing ability. Fig. 17 illustrates a focusing of the pulse

$$w(z,t) = \int\limits_{-\infty}^{\infty} a(\kappa) \frac{e^{i(\sqrt{\kappa^2-\Phi^2}z-\kappa t)}}{\sqrt{\kappa^2-\Phi^2}} d\kappa$$

with function $a(\kappa)$ given by (21). The field $U(g;t) = -e^{i\Phi y}/(2i)^{-1} w(z,t)$ caused by the pulse may be thought of as a field of the located in the plane $z = 0$ the point source $F(g;t) = e^{i\Phi y}\delta(z)f(t)$; $f(t) = 0$ at $t < 0$. Hence function $U(g;t)$ is a solution of initial boundary value problem (10)–(12) with $\varepsilon = 1$, $S = \emptyset$, $\varphi(g) = \Psi(g) \equiv 0$ and

$$f(t) = \int\limits_{-\infty}^{\infty} a(\kappa) e^{-i\kappa t} d\kappa. \tag{25}$$

To be certain, one only needs to put spectral representation (25) in the problem solution (see [6])

$$U(g;t) = -\frac{e^{i\Phi y}}{2} \int\limits_{0}^{t-z} J_0\left(\Phi\sqrt{(t-\tau)^2 - z^2}\right) f(\tau) d\tau. \tag{26}$$

4. Let $w(0,t) = \delta(t)$. Then in view (18),

$$w(z,t) = \delta(t-z) - \Phi z \frac{J_1(\Phi\sqrt{t^2-z^2})}{\sqrt{t^2-z^2}} \chi(t-z).$$

The unaffected pulse propagating at the speed of light is followed by an oscillating tale. In $t-z$ coordinates, these oscillations rise in amplitude

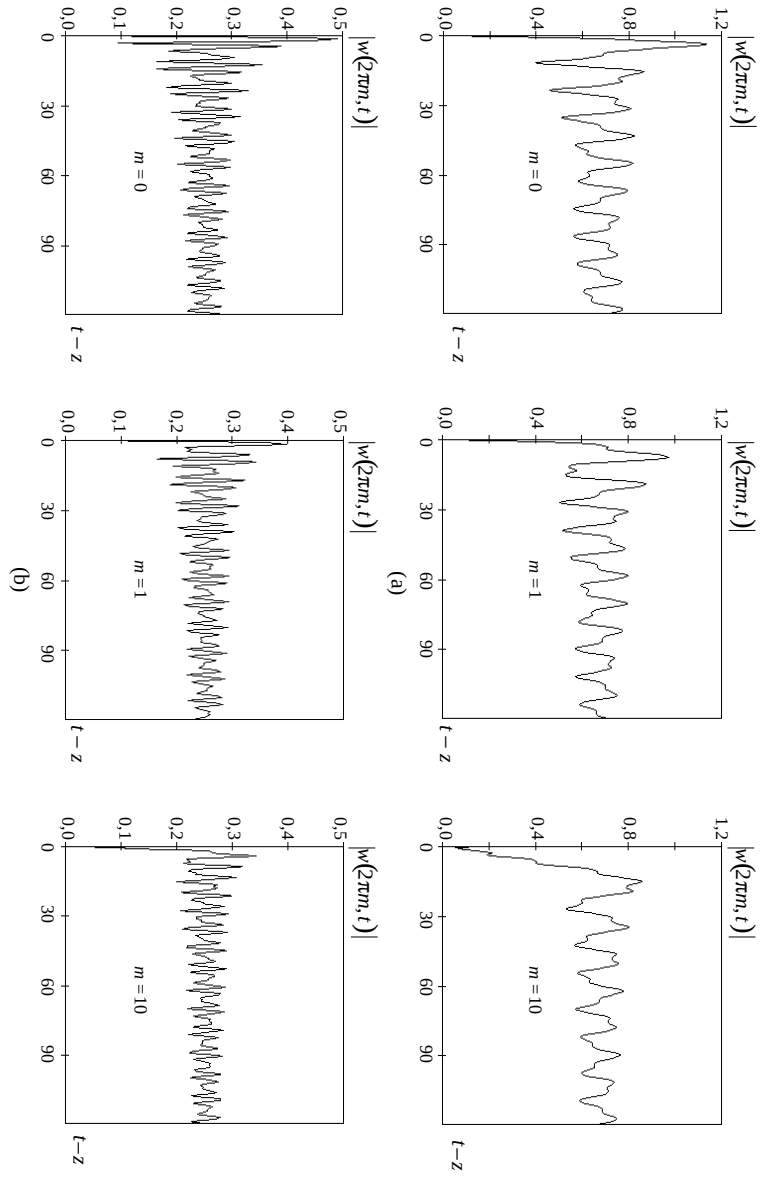

Figure 21. Wave, propagating from constantly (starting at moment $t = 0$) operating source: $F(g;t) = e^{i\Phi y}\delta(z)f(t)$; $f(t) = e^{-i\tilde{\kappa}t}$, $t > 0$ and $f(t) = 0$, $t \leq 0$; $\Phi = 0.3$. (a) $\tilde{\kappa} = 0.8$; (b) $\tilde{\kappa} = 2$.

and frequency as the propagation distance increases. The first peak of the tail amplitude envelope gradually overtakes the original δ-pulse. The rest ones, which line up at progressively shorter distances, follow the first peak. The signal gets much distortion, mainly owing to that the local amplitudes centers of the tail-forming "pulses" move faster than light. The similar effects likely attend the propagation of all broad band pulses with non analytic envelope. Unlike the δ-pulse case, there appears an additional danger that the forerunner would be much distorted at the moment when the local amplitude centers of the tail overtake the amplitude center of the pulse starting from the plane $z = 0$. The said is verified, in particular in Fig. 18 — the effective frequency band occupied by the pulses lies in the domain $[\tilde{\kappa} - 3, \tilde{\kappa} + 3]$ which involves the threshold points $\kappa = 0.3$ (Fig. 18a) and $=0$ (Fig. 18b) which split the spectral domain into sub domains with essentially different propagation conditions.

The analogous phenomena are also inherent to broad band pulses with qubic phase modulation (see Fig. 19). When modulation coefficient γ is sufficiently large in modulus, the principal part gets splitting, and the newly formed amplitude centers either overtake ($\gamma > 0$) the principal one or lag behind it ($\gamma < 0$).

The quadratic phase modulation of an broad band pulse with analytic envelope in the frequency domain influences the propagation process as well as it does in the case of narrow band signals (see Fig. 20; the focusing process performed as before at a positive β is thoroughly considered in Fig. 20c, lower plot).

In closing, one more example is offered. Fig. 21 illustrates the propagation of wave $U(g;t) = w(z,t)e^{i\Phi y}$ arising due to the distributed in the plane $z = 0$ source $F(g;t) = e^{i\Phi y}\delta(z)e^{-i\tilde{\kappa}t}\chi(t)$. The envelope whose structure is determined by a stepwise character of the excitation function is subject to the superimposition of oscillations with frequency $\tilde{\kappa}$. The greater $\tilde{\kappa}$ is, the sooner and at a shorter distance comes the process to the proper quasi harmonic mode.

Particular attention should be given to the case $\tilde{\kappa} = \Phi$ when the excitation frequency $\tilde{\kappa}$ coincides with one of the real eigen frequencies $\overline{\kappa}$ of the regular Floquet channel [1]. From (26) at $z = 0$ one obtains the representation

$$w(0,t) = -\frac{1}{2}\int_0^t J_0\left[\tilde{\kappa}(t-\tau)\right] e^{-i\tilde{\kappa}\tau} d\tau = -\frac{1}{2} t\left[J_0(\tilde{\kappa}t) - iJ_1(\tilde{\kappa}t)\right]$$

which is no longer at the level of late-time asymptotic but in a literal sense in the pure state demonstrates all the characteristic features of the energy store process in the near field (see part 5, item 2).

7. CONCLUSION

In this paper we have attach much importance to the understanding of the fundamental phenomena accompanying this process being inspired by the paper [8] which for the last decades has been one of the most significant, offering an exhaustive analytical treatment of the pulse deformations when propagating in regular lines. A complete analytical solution of the problem is not available yet, and a comprehensive numerical study with a proper interpretation of the results is only expected to be of help.

Resonance inhomogeneities in the propagation domain essentially complicate a physical picture of the process and make the analysis all the more problematic. But even a bit of the reliable information may make up the basis for the creation of fundamentally new units and devices as well as for the development of contemporary theory of resonant wave scattering.

The presented approach relies on the well-known mathematical concept of the analytical continuation of a complex function of real variable into the domain of complex-valued argument. On this basis, in the IRE NAS of Ukraine a contemporary FD theory of resonance wave scattering by gratings and waveguide inhomogeneities has been developed [1–3, 7] to be recognized as a groundwork for the analysis of resonance scattering in the time domain.

Our experience confirms statements [8] that it is not necessary to consider arbitrary media and lines. The analysis should be always related to particular real parameters and characteristics of the propagation media and waveguide circuits, since many special features in the processes of pulse scattering and propagation are caused by unimportant at first glance details (see, for instance, [11] where sea water is used for the propagation medium). Our investigation has been concerned with signals formed by classical one- dimensional periodic structures and with their scattering and propagation in regular and irregular segments of the Floquet channel. Of course, the revealed phenomena cannot cover the whole spectrum of possible anomalous and, in a sense, regular space-time transformations of the electromagnetic field. So we hope and plan to gain better insight in our further work.

REFERENCES

1. Shestopalov, V. P. and Y. K. Sirenko, *Dynamical Theory of Gratings,* 214, Naukova Dumka, Kiev, 1989 (in Russian).
2. Shestopalov, V. P., L. N. Litvinenko, S. A. Masalov, and

V. G. Sologub, *Diffraction of Waves on Gratings,* 278, Kharkov State University Publishers, Kharkov, 1973 (in Russian).

3. Shestopalov, V. P., A. A. Kirilenko, and S. A. Masalov, *Matrix Equations of Convolution Type in the Diffraction Theory,* 293, Naukova Dumka, Kiev, 1984 (in Russian).
4. Perov, A. O., Yu. K. Sirenko, and N. P. Yashina, "Explicit conditions for virtual boundaries in initial boundary, value problems of the wave scattering theory," *Journal of Electromagnetic Waves and Applications,* Vol. 13, No. 10, 1343–1371, 1999.
5. Sirenko, Yu. K. and N. P. Yashina, "Nonstationary model problems for waveguide open resonator theory," *Electromagnetics,* Vol. 19, No. 5, 419–442, 1999.
6. Perov, A. O. and Yu. K. Sirenko, "Nonstationary model problems of electrodynamical theory of gratings," *Radiophysica i Electronica,* Vol. 2, No. 2, 66–86, IRE NAN of Ukraine, Kharkov, 1997 (in Russian).
7. Shestopalov, V. P., A. A. Kirilenko, S. A. Masalov, and Yu. K. Sirenko, *Resonant Scattering of Waves. V.1. Diffraction Gratings,* 232, Naukova Dumka, Kiev, 1986 (in Russian).
8. Vainshtein, L. A, "Propagation of pulses," *Speech Fizicheskih Nauk,* Vol. 118, 339–367, 1976 (in Russian).
9. Ladyzhenskaya, O. A, *The Boundary Value Problems of Mathematical Physics,* 407, Springer-Verlag, New York, 1985.
10. Bliokh, P. B., "Compression of a radiation pulse in depressive medium with random inhomogeneities," *Izvestiya VUZov. Radiofizika,* Vol. 7, No. 3, 460–470, 1964 (in Russian).
11. King, R. W. P., "The propagation of a Gaussian pulse in sea water and its application to remote sensing," *IEEE Trans. On Geoscience and Remote Sensing,* Vol .31, No. 3, 595–605, 1993.

Andrey O. Perov graduated from the Mechanics and Mathematics Faculty of Kharkov State University in 1994. Majored in applied mathematics. Since 1994 he is researcher in staff of the Institute of Radiophysics and Electronics of Sciences of Ukraine, where he is now working towards his Ph.D. His scientific interests are analytical and numerical techniques for wave motion process simulation and resonant phenomena.

Yury K. Sirenko Received Candidate and Doctor of Science degrees in Physics and Mathematics from Kharkov State University, Ukraine, in 1978 and 1988, respectively. Since 1974 he has been the staff of

the Institute of Radiophysics and Electronics of National Academy of Sciences of Ukraine as post-graduate student, researcher, senior researcher, and head of the Department of Wave Scattering Theory. Since 1989 he has been a Professor of Mechanics and Mathematics Faculty of Kharkov State University. His current research activities are focused on mathematical simulation in applied electromagnetics.

Nataliya P. Yashina received a Candidate of Science degree in Physics and Mathematics from Kharkov State University, Ukraine, in 1979. In 1973 she joint the Department of Mathematical Theory of Diffraction in the Institute of Radiophysics and Electronics of National Academy of Sciences of Ukraine as graduate student. Now she is a senior researcher of the Institute. In 1996–1998 she was with Gebze Institute of Technology, Turkey as associate professor. Her interest are in analytical and numerical methods of diffraction theory, resonant scattering in waveguides.